

Data Descriptor

Title

Hydrologic outputs generated with the 2023 calibrated version of GEM-Hydro over the Great-Lakes.

Authors

Étienne Gaborit¹, Juliane Mai^{2,3,4}, Daniel Princz⁵, Hongren Shen⁶, Vincent Vionnet¹, Bryan Tolson⁶, and Vincent Fortin¹

Affiliations

1. Meteorological Research Division, Environment and Climate Change Canada, QC, Canada
2. While at: Computational Hydrosystems, Helmholtz Centre for Environmental Research – Leipzig, Germany
3. While at: Center for Scalable Data Analytics and Artificial Intelligence – Leipzig, Germany
4. Now at: Department of Earth and Environmental Science, University of Waterloo, ON, Canada
5. National Hydrologic Services, Environment and Climate Change Canada, SA, Canada
6. Department of Civil and Environmental Engineering, University of Waterloo, ON, Canada

corresponding author(s): Étienne Gaborit (Etienne.Gaborit@ec.gc.ca)

Abstract

The dataset described in this document contains outputs from a calibrated version of the GEM-Hydro hydrologic model developed at Environment and Climate Change Canada (ECCC), over the Great Lakes and Ottawa river basins, and for the period 2001-2018 included. This dataset is available on the Federated Research Data Repository.

The outputs consist of all variables (hourly fluxes and state variables) related to the water balance of the land-surface scheme of GEM-Hydro, as well as mean daily streamflow time-series (observed and simulated) at 212 gauge stations within the region of interest.

To produce these outputs, a calibrated version of the GEM-Hydro model was run in open-loop mode (no land-surface or streamflow assimilation performed), driven with atmospheric forcings coming from the ECCC Canadian Surface Reanalysis (CaSR version 2.1).

GEM-Hydro is shown here to be able to perform satisfactory simulations of various hydrologic variables, when compared to reference datasets. The hydrologic variables of this dataset include precipitation, surface runoff, sub-surface runoff (soil lateral flow), soil base drainage, evapo-transpiration, snow water equivalent, soil moisture content for 6 soil layers down to 2m, water stored in the vegetation canopy, and streamflow.

These variables can be used for example to run and calibrate any routing model, compute climatologies, various statistics, or trends for different hydrologic variables over the region of interest, assess the variability of these variables as a function of the local geo-morphology, etc.

Background & Summary

The Great-Lakes basin is a transboundary watershed between the U.S.A. and Canada. It is the largest surface freshwater system on Earth and is home to 37 million people. Together with the Ottawa River basin, they represent a total drainage area of about 965 000 km². This system is crucial in terms of freshwater resources. For water resource management and in the context of climate change, it is important to understand the main processes governing the different water balance components in the region, as well as their spatial and temporal

52 variability. Despite observations are being available for several components of the water
53 balance, most of these observations only consist of in-situ measurements, which can be sparse
54 both in space and time while being rarely co-located between various variables observed.
55 Physically-based, distributed hydrologic models can, however, produce consistent, seamless,
56 and continuous (both in space and time) simulations of the different terms of the water
57 balance equation, with a relatively detailed spatial and temporal resolution. These models can
58 also be applied for various applications, such as scenario testing or climate-change impact
59 assessment.

60 GEM-Hydro (Gaborit et al. 2017¹, Vionnet et al. 2020²) is a physically-based,
61 distributed hydrologic model developed at Environment and Climate Change Canada (ECCC).
62 This model is used inside the National Surface and River Prediction System (NSRPS, see
63 Durnford et al. 2021³: poster available at
64 <https://ams.confex.com/ams/101ANNUAL/meetingapp.cgi/Paper/383559>). The NSRPS is
65 used at ECCC to perform real-time surface and hydrologic analyses and forecasts, both
66 deterministic and probabilistic, over Canada and the main US/Canada transboundary
67 watersheds.

68 So far, the GEM-Hydro version used in NSRPS is the “default” version of the model, in
69 the sense that none of its internal parameters were calibrated to maximize streamflow or
70 other variables’ performances. Despite the default version of GEM-Hydro can have very
71 satisfactory performances in some areas, it can also show very limited performances in others.
72 Agricultural areas are a good example of regions where the default GEM-Hydro version has
73 limited performances with regard to streamflow simulations, because tile drains that are
74 generally installed in such areas to drain any excess of water, are not explicitly represented in
75 the model. Despite the model being physically-based, it cannot accurately represent all the
76 physical processes unfolding in reality (Baroni et al. 2019⁴, Budhathoki et al. 2020⁵). Moreover,
77 there are not enough field observations to accurately parameterize the model in all areas of a
78 given domain (Hirpa et al. 2018⁶). Finally, even physically-based models still rely on empirical
79 or conceptual relationships in some parts of the model (Mai 2023⁷), for example to translate
80 soil texture information into soil hydraulic conductivities. For all these reasons, any hydrologic
81 model still needs calibration to achieve its best performances, as illustrated by many recent
82 studies, such as, for example, those of Budhathoki et al. (2020⁵), Hirpa et al. (2018⁶), Bajracharya
83 et al. (2023⁸), Mai 2023⁷, Mei et al. 2023⁹, and Demirel et al. 2024¹⁰, among many others.

84 GEM-Hydro has already been calibrated in the past (see Gaborit et al. 2017¹, Mai et
85 al. 2021¹¹, Mai et al. 2022¹²) for research purposes, mainly as part of the different Great Lakes
86 Runoff Intercomparison Projects (GRIP). During these projects, the tools and methodology
87 used to calibrate GEM-Hydro have continuously evolved. For example, the routing component
88 of GEM-Hydro was replaced during calibration with a simple Unit Hydrograph technique in
89 Gaborit et al. 2017¹ to save computation time, while it was implemented in Mai et al. 2021¹¹
90 with a coarse 10-km resolution, before being replaced in Mai et al. 2022¹² by the Raven routing
91 model (still to save computation time). Even after the most recent GRIP project that focused
92 on the whole Great-Lakes region (GRIP-GL, see Mai et al. 2022¹²), improvements were needed
93 to further improve the GEM-Hydro calibration, mainly with regard to surface soil moisture
94 (SSM) in the Lake Erie and Ottawa River basins, and with regard to evapo-transpiration (ET)
95 and snow water equivalent (SWE) in the Ottawa River basin.

96 The GEM-Hydro outputs shared in the dataset presented here are published on the
97 Federated Research Data Repository (FRDR; Gaborit 2024¹³) and were produced with the most
98 recent calibrated version of GEM-Hydro (referred to as the 2023 calibrated version), at the
99 time of writing. This 2023 calibrated version was obtained by following generally the same
100 calibration methodology as the one used in the GRIP-GL project (see Mai et al. 2022¹² and its
101 supplements for more details), but with several significant differences compared to it. The
102 methodology employed to produce the 2023 calibrated version is explained in detail in the
103 Methods section, but a brief summary of the four main steps involved is presented further

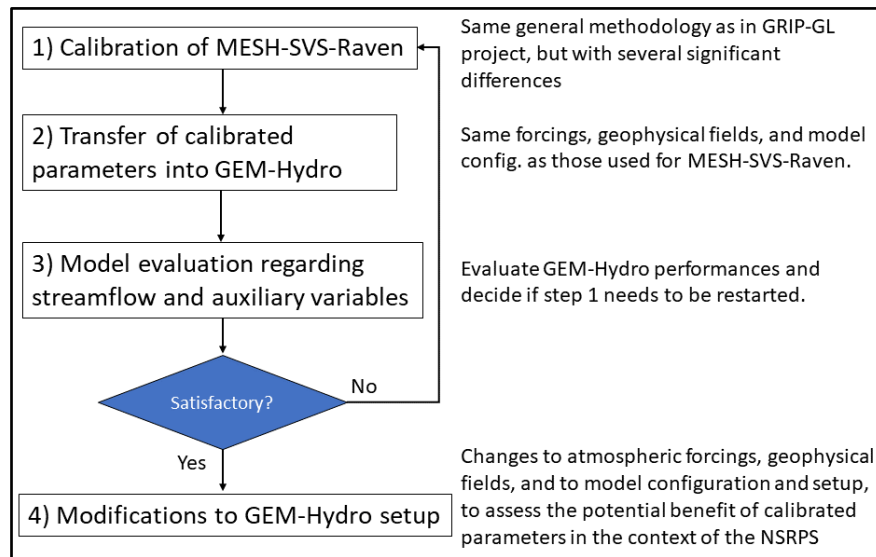
104 down and in Figure 1. However, a brief overview of the GEM-Hydro model is given first, as it
105 may help the reader to better understand the general strategy used here to calibrate GEM-
106 Hydro.

107 The GEM-Hydro model is composed of two main components. The first one is GEM-
108 Surf (Bernier et al. 2011¹⁴), which is the surface component of the model. It can represent up
109 to 5 different types of surface covers (or tiles) inside each grid cell, i.e., glaciers, land, water,
110 frozen water, and urban areas. Over land, GEM-Hydro relies on the Soil, Vegetation and Snow
111 (SVS) land-surface scheme (Alavi et al. 2016¹⁵, Husain et al. 2016¹⁶, Leonardini et al. 2020¹⁷,
112 2021¹⁸). SVS represents two types of snow-free covers, i.e., high and short vegetation, , and
113 bare ground. In winter, it represents two different snowpacks, i.e., snow over bare ground and
114 short vegetation, and snow under high vegetation. SVS represents a single soil column made
115 of several layers (generally 7, that go down to a 3-m depth). The second GEM-Hydro
116 component is WATROUTE (Kouwen 2010¹⁹), which is the routing component of the model that
117 is used to convey water in the network of lakes and rivers and to simulate streamflow.
118 WATROUTE is a gridded routing model implemented with a 1-km resolution in GEM-Hydro. It
119 can represent lakes and reservoirs, as well as diversions. To represent regulated reservoirs,
120 WATROUTE relies on the Dynamically Zoned Target Release (DZTR) reservoir model (Yassin et
121 al. 2019²⁰, Gaborit et al. 2022²¹). Watroute simulates baseflow (the contribution of the aquifers
122 to the surface network) using a conceptual reservoir in each grid-cell, called the Lower Zone
123 Storage (LZS), which is fed with drainage from GEM-Surf and estimates baseflow based on a
124 power function. In GEM-Hydro, GEM-Surf and WATROUTE are one-way coupled, meaning that
125 the routing scheme has no impact on the surface component.

126 GEM-Hydro is computationally expensive, which is generally the case for physically-
127 based distributed hydrologic models, when implemented over large scales (Baroni et al.
128 2019⁴). Therefore, when it comes to calibration, where many simulations are required over
129 relatively long time periods, the model's computational time can become a strong limitation
130 for the calibration exercise (see for example Hirpa et al. 2018⁶). In the case of GEM-Hydro, the
131 model is not directly usable for calibration purposes when implemented over large regions,
132 such as the one considered here. The two main reasons for the high computational time of
133 GEM-Hydro are that the surface component runs using successive 24-h integration cycles (a
134 lot of time is spent in input/output processing), and that the routing scheme is gridded,
135 implemented at a 1-km resolution, and not parallelized (all grid points are processed in a
136 sequential manner from the most upstream points to the outlet).

137 Therefore, the "Modélisation Environnementale communautaire - Surface et
138 Hydrologie" platform (MESH, see Pietroniro et al. 2007²²) including the SVS land-surface
139 scheme, along with the Raven routing model (Craig et al. 2020²³) is used for the calibration
140 instead (hereafter referred to as MESH-SVS-Raven). This corresponds to the first step of the
141 general methodology employed here (see Figure 1). MESH-SVS is faster to run compared to
142 the surface component of GEM-Hydro; mainly because it runs over a given time period using
143 a single integration, i.e., not stopping and restarting each day like GEM-Hydro does. Raven
144 routing is much faster than WATROUTE (see Mai et al. 2022¹²) because Raven routing is vector-
145 based, while WATROUTE is a grid-based routing model implemented with a high resolution
146 (1km). The calibrated parameters obtained with MESH-SVS-Raven are then transferred into
147 the actual GEM-Hydro model (step 2 of Figure 1). For these first two steps, the atmospheric
148 forcings, geophysical fields, model configuration, etc. for both the GEM-Hydro and MESH-SVS-
149 Raven models were exactly the same as those used in the GRIP-GL project (Mai et al. 2022¹²).
150 This was done in order to be able to assess the benefit of the changes employed here for the
151 GEM-Hydro calibration methodology, when compared to the one employed during GRIP-GL
152 (see next section). After the second step, a comprehensive evaluation of the calibrated GEM-
153 Hydro version was performed including streamflow performances, but also auxiliary
154 hydrologic variables and near-surface meteorological variables (see "Technical Validation"
155 section). This was done to ensure that the calibration exercise performed here by only

156 maximizing streamflow performances (see “Methods” section) did not degrade other
 157 hydrologic variables. If this was the case, changes were then brought to the calibration
 158 methodology (see “Methods”) and step 1 was restarted (see Figure 1). After a total of six
 159 iterative calibration experiments performed during this study, the resulting GEM-Hydro
 160 performances were judged satisfactory, and step 4 was performed (Figure 1). During step 4,
 161 the GEM-Hydro setup using the calibrated parameters was modified to use a setup that is close
 162 to the one employed in the operational version of NSRPS. This was done to assess the benefit
 163 that this calibration exercise could ultimately bring to ECCC’s operational surface and rivers’
 164 analyses and forecasts.
 165



166

167 *Figure 1: general workflow employed to calibrate some GEM-Hydro model parameters and use them in a setup that*
 168 *is close to the one used in the National Surface and River Prediction System (NSRPS). Note that the setup of step 4*
 169 *is the one used to produce the outputs that are shared and described in this document.*

170

171 The GEM-Hydro outputs shared in this dataset were obtained from step 4 of Figure 1,
 172 which involves using a setup that is close to the one employed in NSRPS. More details can be
 173 found in next section. It is important to note that to produce these outputs, the calibrated
 174 version of the GEM-Hydro model was run in open-loop mode (no land-surface or streamflow
 175 assimilation performed), driven by atmospheric forcings coming from version 2.1 of the
 176 Canadian Surface Reanalysis (CaSR), which relies on the Regional Deterministic Reforecast
 177 System (RDRS, see Gasset et al. 2021²⁴). Therefore, even if no assimilation was performed for
 178 any surface variable or streamflow during these calibrated GEM-Hydro runs, they were forced
 179 with atmospheric forcings that come from a reanalysis. This means that, for example,
 180 precipitation forcings correspond to precipitation analyses, which consist of short-term
 181 forecasted precipitation fields corrected by various sources of precipitation observations. The
 182 fact that no assimilation was performed in these GEM-Hydro runs has advantages. For
 183 example, the mass of water is conserved in these simulations (from total grid cell precipitation
 184 to total streamflow leaving a watershed), whereas the general water balance can be
 185 significantly altered in the case of data assimilation, potentially leading to a decrease in model
 186 performance regarding streamflow simulations (see for example Garnaud et al. 2021²⁵).
 187 Another advantage is that without data assimilation, the physical link between the different
 188 simulated hydrologic variables is preserved, allowing for example to analyse the
 189 characteristics of the relationship between these hydrologic variables.

190 The outputs shared in this dataset consist of all variables (hourly fluxes and state
191 variables) related to the SVS water balance (land-surface scheme of GEM-Hydro), as well as
192 mean daily streamflow time-series (observed data and simulated data using WATROUTE), at
193 gauge locations across the region of interest. The land surface variables comprise
194 precipitation, surface runoff, sub-surface runoff (soil lateral flow), soil base drainage, evapo-
195 transpiration (ET), snow water equivalent (SWE), soil moisture (SM) content for 6 soil layers
196 down to 2 m, and water stored in the vegetation canopy. The outputs are provided over the
197 Great-Lakes and Ottawa River basins, and over the period from January 2001 to December
198 2018. The variables can be used, for example, to run and calibrate any routing model, compute
199 climatology, various statistics, or trends for different hydrologic variables over the region of
200 interest, assess the variability of these variables as a function of the local geo-morphology, etc.

201 As part of the GRIP-GL project (Mai et al. 2022¹²), GEM-Hydro was often the best
202 model regarding SWE and surface SM (SSM) simulations, when compared to other conceptual
203 and lumped models, or to other distributed and physically-based models widely used in North
204 America, but the version presented here is even better regarding these variables. Therefore,
205 it is argued that the hydrologic variables shared in this dataset can be useful to a broad variety
206 of users of the hydrologic community.

207

208 **Methods**

209

210 1) Calibration

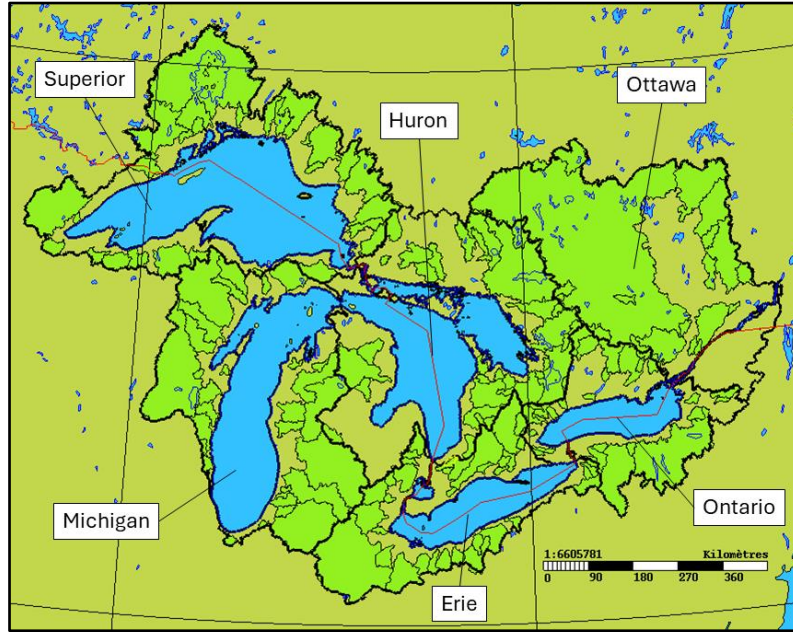
211

212 **1.1 – Similarities with the GRIP-GL calibration methodology.**

213

214 The general GEM-Hydro calibration methodology employed here is the same as in GRIP-
215 GL (see Mai et al. 2022¹²) and includes the main steps described hereafter. MESH-SVS-Raven
216 is used during the calibration exercise in place of GEM-Hydro, to save computation time (see
217 “Background and Summary”). The same geophysical fields and forcings as those used in the
218 GRIP-GL project (Mai et al. 2022¹²) were used with MESH-SVS-Raven during the calibration
219 exercise performed here. The forcings come from the version 2.0 of the Canadian Surface
220 Reanalysis (CaSR), which relies on the Regional Deterministic Reforecast System v2.0 (RDRS,
221 see Gasset et al. 2021²⁴). All model runs (i.e., both MESH-SVS-Raven and GEM-Hydro
222 simulations) started on January 1st, 2000, and were initialized with GEM-Hydro outputs
223 corresponding to January 1st of 2014. These GEM-Hydro outputs are the result of an open-loop
224 run of the default version of the model, over multiple years (from 2000 to 2014). The year
225 2000 was considered a spinup period for the model runs, and was not used for evaluation
226 (outputs are not shared for this spinup year in the dataset described here).

227 A global calibration approach (Gaborit et al., 2015²⁶, Demirel et al. 2024¹⁰) is used for
228 each of the six main subdomains of the region of interest. There is a subdomain for each
229 specific watershed of the five Great Lakes, plus the watershed of the Ottawa River, as shown
230 on Figure 2. This means that the performances at all flow gauges located inside a given
231 subdomain are considered as a whole, at once, for example using the median or the mean of
232 the different stations' performances. The only variable being considered to compute the
233 objective function for a given subdomain is the mean daily streamflow at flow gauges of this
234 subdomain. This strategy of using a global calibration for each of the different subdomains is
235 also referred to as "regional calibration" (Mai et al. 2022¹²), or as “multi-basin calibration”
236 (Demirel et al. 2024¹⁰). Figure 2 presents the 6 main subdomains and the 212 basins
237 considered in the region.



239

240 *Figure 2: The delineation of the six main subdomains considered here (the 5 Great-Lakes watersheds and the*
 241 *Ottawa River basin), along with the subbasins of the 212 flow gauges used in this study (light green).*

242 The Dynamically Dimensioned Search (DDS) calibration algorithm (Tolson and Shoemaker
 243 2007²⁷) is used with a maximum of 240 iterations to perform the calibration of MESH-SVS-
 244 Raven. Indeed, DDS is known for its fast convergence (Mai 2023⁷). Moreover, when looking at
 245 the evolution of the objective function as a function of the number of iterations during
 246 calibration, for any calibration experiment performed in this study, it was clear that the
 247 objective function reached an asymptotical behaviour before the maximum number of 240
 248 iterations allowed here (not shown). Note, however, that this number may be insufficient in
 249 other calibration contexts.

250 The calibration parameters mostly consist of multiplying coefficients that are used to
 251 multiply the actual model parameters (that generally vary in space) the same way to preserve
 252 their original spatial variability. The original actual model parameter values are computed by
 253 default by the model (SVS or Raven) based on the geophysical fields provided as input to the
 254 models. See Table 1 for information about the multiplying coefficients used as calibration
 255 parameters during this work. Moreover, some constraints were applied to the adjusted
 256 parameter values actually used in the model, to make sure that the modified values would
 257 remain physically coherent. For example, the final albedo values were capped to 1.0, and the
 258 final 50% root depth (see table 1) was constrained to remain between a minimal value of 1
 259 cm, and a maximal value of 2cm below the 95% root depth.

260

261 *Table 1: List of the calibration parameters used, along with a short definition. Init.: Initial value; low,high: lower and*
 262 *upper limits of the interval allowed for a given parameter during calibration. Horiz.: Horizontal; Hydraul.: hydraulic;*
 263 *Cond.: Conductivity; coeff.: coefficient; Agric.: agricultural; LZS: Lower Zone Storage; UH: Unit Hydrograph. See text*
 264 *for the justification of interval limits used for some parameters.*

MESH-SVS
parameters

	Init.	low	high	Parameter definition
MLTM	1	0.8	1.1	snowmelt rate divider
GRKMOD	1	1	2.5	horiz. hydraul. Cond. multiplier (all soil layers, non-agric. areas)
GRKMO_A	1	1	100	horiz. hydraul. Cond. multiplier (layer 5, agric. areas)
KASMOD	1	1	2.5	vert. hydraul. Cond. multiplier (all soil layers, non-agric. Areas)
KASMO_A	1	1	5.0	vert. hydraul. Cond. multiplier (first 3 soil layers, agric. areas)
EVMOD	1	0.8	1.5	evapo-transpiration resistance multiplier

SUMOD	1	0.7	1.2	sublimation resistance multiplier
RTMOD	1	1	1.5	95% and 100% root depth multiplier
DMOD	1	0.7	1.1	50% root depth multiplier
AMOD	1	1	1.2	albedo multiplier
URMO	1	1	1.3	urban area impervious fraction multiplier
FLZCOEFF	2.40E-05	1.00E-07	1.00E-03	LZS multiplicative coeff.
PWRC	2.8	2	4	LZS power coeff.
R1NC	1	0.5	2	Mannings' coeff. Multiplier
GASH	1	0.5	2	Multiplier of the shape of the gamma UH
GASC	1	0.5	2	Multiplier of the scale of the gamma UH
LACRWD	1	0.1	1	lake outlet width multiplier

265

266

267 **1.2 – Differences with regard to the GRIP-GL calibration methodology.**

268

269 The differences of the methodology employed here to calibrate GEM-Hydro, as
 270 compared to the one used in GRIP-GL, include the following changes. Some bugs related to
 271 the reading of some geophysical fields in MESH-SVS were corrected (see Mai et al., 2022¹²).
 272 Because of these bugs, the calibrated parameter values obtained during GRIP-GL were not
 273 optimal for GEM-Hydro, leading to a significant drop of performances between MESH-SVS-
 274 Raven and GEM-Hydro. Since the bugs have been fixed, the performances between the two
 275 systems are much closer, as can be seen in the “technical validation” section.

276

277 All flow stations used in the GRIP-GL project were used here for calibration, except a
 278 few ones. In opposition to the GRIP-GL project, where some stations were not used during
 279 calibration in order to perform a spatial validation of the calibrated models, as many stations
 280 as possible were used here during calibration. This was done in order for the objective function
 281 to be as representative as possible of the performances for all parts of a given subdomain.
 282 Moreover, it was not necessary to keep stations for the spatial validation of the model, since
 283 the spatial robustness of the calibration methodology employed here has already been
 284 demonstrated during the GRIP-GL project (Mai et al. 2022¹²). However, some stations were
 285 still discarded during calibration. Indeed, some of the basins considered here have a heavily
 286 regulated flow regime, while this regulation was not explicitly represented in the Raven setup
 287 used here, resulting for some of these stations in poor model performances with the default
 288 version of MESH-SVS-Raven. Therefore, it was necessary to discard these basins during
 289 calibration, otherwise they could have misguided the evolution of the calibration algorithm.
 290 However, not all basins involving flow regulation were excluded during calibration, because in
 291 some cases the impact of the regulation did not prevent the default version of MESH-SVS-
 292 Raven from achieving satisfactory simulations. This is the case for example for the station
 293 02KF005 (Ottawa River at Britannia): despite the basin includes about 12 major dams, the
 294 regulation still has a limited impact on the total flow of the watershed (especially in spring),
 295 due to its large size (90 900 km²). The list of stations that were excluded from the calibration
 296 exercise performed here can be found in Table 2. However, note that all stations were
 297 considered when comparing the default and calibrated versions of the GEM-Hydro model (see
 298 “Technical validation”). Indeed, many major dams of the Great-Lakes and Ottawa River basins
 299 are explicitly represented with the DZTR model, in the WATROUTE routing component of GEM-
 300 Hydro. The complete list of the 212 flow stations considered in this study, along with their
 301 main basin characteristics, can be found in Mai et al. (2022¹²).

301

302 *Table 2: list of stations not considered during calibration, along with their (revised) Kling-Gupta Efficiency (KGE, see*
 303 *Kling et al. 2012²²) performances over the period 2001-2010 for the default version of MESH-SVS-Raven, and the*
 304 *default and calibrated versions of the GEM-Hydro model. The stations highlighted in green are those for which the*

305
306

regulation is explicitly represented in GEM-Hydro using the DZTR model (Yassin et al. 2019²⁰). Note that in the MESH-SVS-Raven setup used here, the DZTR model was not used, for any stations.

Subdomain	Station ID	Watershed size (km ²)	MESH-SVS-Raven	GEM-Hydro default	GEM-Hydro calibrated
Huron	02EB011	4790	-1.58	0.35	0.52
Huron	02DD010	13900	0.47	0.63	0.63
Huron	02DB005	3150	0.11	0.3	0.36
Huron	04136000	2870	-0.44	-1.41	-0.59
Huron	04137500	4500	-0.77	-1.67	-0.81
Ont	02HF002	1280	-0.02	0	-0.2
Ott	02LE025	883	-0.11	0.02	0.08
Sup	02AD012	24700	0.42	0.75	0.7
Sup	02BD002	5310	-0.1	-0.1	-0.35
Sup	02BD007	1950	0.13	0.21	0.01
Sup	02BE002	2880	-0.31	-0.24	-0.48
Sup	04044724	210	0.32	0.05	-0.07
Median of the five "green" stations			0.11	0.35	0.52
Median of other stations			-0.10	-0.10	-0.35

307 For each subdomain, the objective function considered during calibration consists of
 308 the mean of the normalized (revised) Kling-Gupta Efficiency (KGE) criteria (see Kling et al.
 309 2012²⁸) across the flow stations of this subdomain. Based on previous calibration experiments
 310 performed, it was preferred to use the mean than the median. When using the median, some
 311 station performances are actually always not reflected in the objective function, resulting into
 312 neglecting their performances. However, when using the mean, all stations' performances are
 313 taken into account in the objective function. Therefore, a normalized version of the (revised)
 314 KGE criteria was required. It corresponds to the revised KGE, but rescaled such that it falls
 315 between 0 and 1. This is done to prevent large negative KGE values obtained for some stations
 316 from strongly affecting the mean, which would put too much emphasis on the worst stations.
 317 In order to normalize the KGE, Equation 1) below was used:

318
$$KGE_n = \frac{1}{2 - KGE} \quad \text{Equation 1), with}$$

319 KGE_n = normalized KGE criteria (values between 0 and 1)

320 KGE = revised KGE criteria (Kling et al. 2012²⁸, values between $-\infty$ and 1).

321

322 The calibration was performed over the period 2008-2017 included (2007 used as spin-
 323 up), and validation period spans over 2001-2007 included (2000 used as spin-up). Using a more
 324 recent calibration period was preferred, given that the calibrated parameters are to be used
 325 ultimately in the NSRPS real-time forecasting system, and given that land use / land cover may
 326 have changed significantly for some areas of the region, over this period of 18 years in total.

327 Some calibration parameters used in GRIP-GL were discarded here because they were too
 328 sensitive on the resulting auxiliary hydrologic variable performances (see "Technical
 329 validation"). The calibration parameters that were included in GRIP-GL but excluded here
 330 consist of the multiplying coefficients related to the three SM content thresholds (wilting
 331 point, field capacity and saturation), the slope of the soil water retention curve, the soil water

332 suction at saturation, the vegetation leaf-area index, and the vegetation roughness (see Mai
 333 et al. 2022¹²). Note that the identification of these problematic parameters was progressively
 334 done during the 6 total iterations of this calibration exercise (see point 2 below). The lower
 335 and upper limits for some parameter intervals mentioned in Table 1 are also different than
 336 the values used in GRIP-GL, because they were also progressively refined during these 6
 337 iterations. The refinement of the parameter intervals that are allowed during calibration was
 338 performed either to prevent unrealistic resulting parameter values in the GEM-Hydro model,
 339 to limit the degradation sometimes noticed for some flow stations or some auxiliary variables
 340 (see Technical validation), or simply to discard some parameter ranges that were never chosen
 341 as the best values by the calibration algorithm, with the objective to prevent the calibration
 342 algorithm to explore useless regions for some parameter values. The latter for example
 343 explains why the lower bound interval limit for some parameters of Table 1 are sometimes
 344 equal to the initial value of 1.0.

345 A new approach to represent the effect of tile drains was employed during calibration: a
 346 specific calibration parameter was used to increase the horizontal hydraulic conductivity of
 347 the SVS soil layer number 5 under agricultural cover, which is located between the depths of
 348 40 and 100 cm, where agricultural tile drains are generally located. This approach to represent
 349 the effect of tile drains in large-scale hydrologic models was suggested by De Schepper et al.
 350 (2015²⁹). However, in SVS, a unique soil column is used, regardless of the type of vegetation
 351 cover. Therefore, a unique multiplying coefficient needs to be used to increase hydraulic
 352 conductivity. This is done by computing a weighted average of two multiplying coefficients,
 353 one specific to agricultural cover, and one specific to covers other than agricultural (see Table
 354 1), as mentioned in Equation 2 below:

355
 356
$$GRKM(I, K) = GRKMOD(I) * (1.0 - FRAC_{A(I)}) + GRKMO_A(I) * FRAC_A(I) \quad \text{Eq. 2), where:}$$

357 $GRKM(I, K)$: final multiplying coefficient used to adjust the soil horizontal hydraulic conductivity of soil
 358 layer K , in grid-cell I . Note that Equation 2 above is only used for $K=5$ (5th soil layer). For the other
 359 layers, $GRKM(I, K) = GRKMOD(I)$

360 $GRKMOD(I)$: multiplying coefficient used to adjust soil horizontal hydraulic conductivity for vegetation
 361 covers other than the agricultural type, in grid-cell I .

362 $FRAC_A(I)$: fraction of the land tile occupied by agricultural cover in current grid cell I .

363 $GRKMO_A(I)$: multiplying coefficient used to adjust soil horizontal hydraulic conductivity for
 364 agricultural vegetation cover, in grid-cell I .

365 Another new approach to represent the effect of ploughing was employed: a specific
 366 calibration parameter was used to increase the vertical hydraulic conductivity under
 367 agricultural cover of the SVS soil layers 1 to 3 (i.e., for depths between 0 and 20 cm, that are
 368 generally strongly impacted by ploughing). However, for the reasons explained above, this
 369 specific coefficient related to agricultural cover needs to be merged with the coefficient
 370 related to other covers, following equation 3) below.

371
$$KASM(I, K) = KASMOD(I) * (1.0 - FRAC_{A(I)}) + KASM_A(I) * FRAC_A(I) \quad \text{Eq. 3), where:}$$

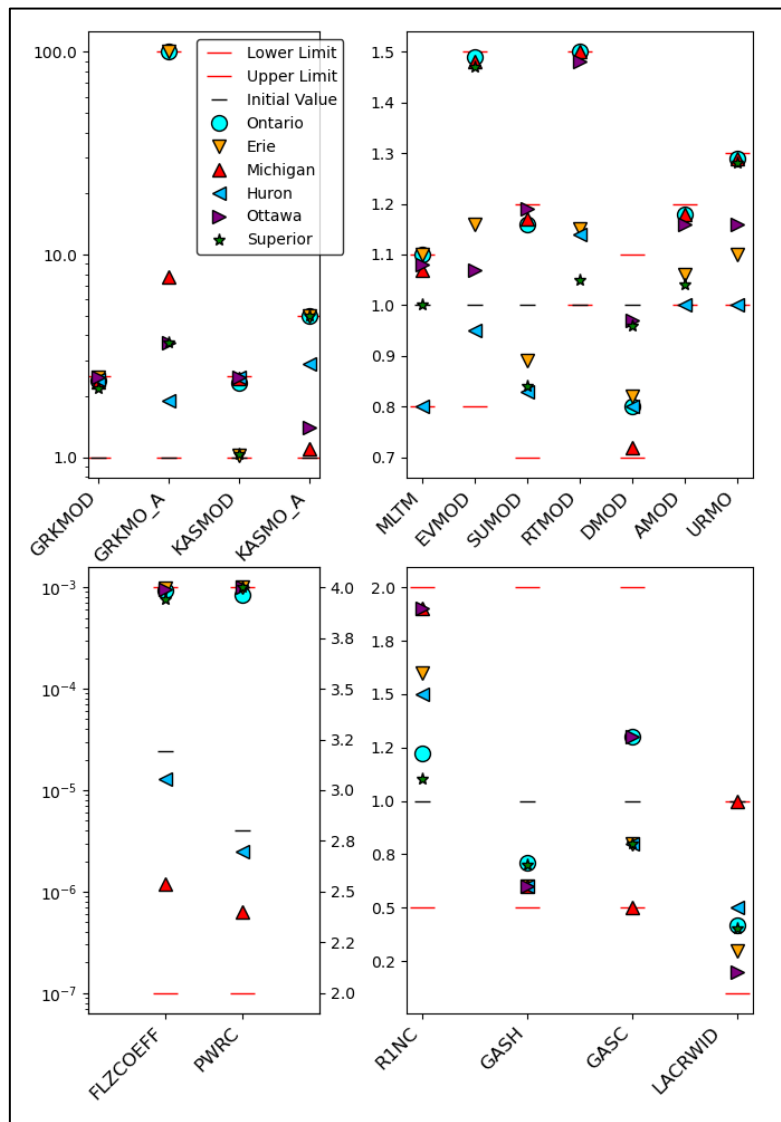
372 $KASM(I, K)$: final multiplying coefficient used to adjust the soil vertical hydraulic conductivity of soil
 373 layer K , in grid-cell I . Note that Equation 3) above is only used for $K = 1$ to 3 (first 3 soil layers). For
 374 the other layers, $KASM(I, K) = KASMOD(I)$

375 $KASMOD(I)$: multiplying coefficient used to adjust the soil vertical hydraulic conductivity for
 376 vegetation covers other than the agricultural type, in grid-cell I .

377 $KASM_A(I)$: multiplying coefficient used to adjust soil vertical hydraulic conductivity for agricultural
 378 vegetation cover, in grid-cell I .

379 *FRAC_A(I)*: fraction of the land tile occupied by agricultural cover in current grid cell *I*.

380 The final values of the calibrated parameters mentioned in Table 1 are shown for the
381 6 different subdomains on Figure 3. It can be seen on Figure 3 that some calibrated parameters
382 exhibit some spatial consistency between the domains regarding their evolution, because they
383 were generally all increased (or decreased) compared to their default value, which is the case
384 for example for GRKMOD, KASMOD, RTMOD, DMOD, R1NC, GASH, and LACRWID. See table 1
385 for a definition of the different calibration parameters. On the opposite, some parameters
386 evolved differently compared to their default value depending on the subdomain, which is the
387 case for MLTM, EVMOD, SUMOD, FLZCOEFF, PWRC, and GASC. In the case of the two
388 parameters related to the LZS (FLZCOEFF and PWRC), their final values for the Lake Huron and
389 Lake Michigan subdomains are very different than those chosen for the other subdomains,
390 which moreover display a very strong coherence between them. This could be the indication
391 of hydrogeologic processes that are specific to the Lake Huron and Lake Michigan subdomains,
392 for example related to the existence of deep (confined) aquifers in these areas. Therefore, the
393 simple LZS conceptual model used in WATROUTE to simulate baseflow may not catch the
394 actual processes occurring for these subdomains in reality, which would probably call for a
395 more complex hydrogeologic model. The fact that the GRKMO_A parameter displays a large
396 spread for calibrated values may be due to the fact that some subdomains contain almost no
397 agricultural areas (like the Lake Huron, Lake Superior and Ottawa River subdomains), making
398 the parameter insensitive during calibration for these domains. This is also probably the case
399 for the URMO parameter related to the impervious degree of urban areas: only the Lake
400 Ontario and Lake Erie subdomains contain basins that are significantly impacted by urban
401 areas. Finally, some parameters reached the upper or lower limit of their allowed interval (see
402 for example GRKMOD, KASMOD, RTMOD, EVMOD, FLZCOEFF or PWRC), but this is the result
403 of the choices made during the six iterations of the calibration trials performed here, as
404 explained above.



405

406 *Figure 3: final calibrated parameter values for each subdomain, along with the initial values and the lower and*
 407 *upper interval limits used for each parameter. The top graphs show the SVS parameters, while the bottom graphs*
 408 *show the calibration parameters for the Raven routing model. See Table 1 for a description of the parameters*
 409 *shown here. Note that for the lower left graph, two different y axes are used.*

410

2) transfer of calibrated parameters into GEM-Hydro

411

Once the calibration was performed with MESH-SVS-Raven, the calibration parameters were transferred into the actual GEM-Hydro model (see step 2 of Figure 1), with no change to the configuration, setup, forcings, etc., such that differences between the calibrated MESH-SVS-Raven and GEM-Hydro models would mainly come from the differences related to the change of the routing model (i.e., from Raven in MESH-SVS-Raven to WATROUTE in GEM-Hydro). This was done in order to ensure that the two different modelling platforms were leading to similar results, and that the calibrated parameters obtained with MESH-SVS-Raven were appropriate for use in GEM-Hydro. See the technical validation section for the differences between MESH-SVS-Raven and GEM-Hydro performances.

420

421

3) Model evaluation regarding streamflow and auxiliary variables

422

At this stage, a comprehensive evaluation of the GEM-Hydro auxiliary hydrologic variables and near-surface variables (SWE, SSM, ET, 2-m temperature and dew point, 10-m wind speed)

423

424 was performed (see Figure 1 and technical validation) in order to make sure that the
425 calibration exercise, only focused on maximizing streamflow performances, did not degrade
426 hydrologic or near-surface variables, when compared to the performances of the default GEM-
427 Hydro version. If this was the case, then the first step of Figure 1 was restarted after changes
428 were brought to the calibration methodology, for example by removing some calibration
429 parameters that were judged too sensitive on the auxiliary hydrologic or near-surface
430 variables, by refining some intervals allowed for calibration parameter values, or by changing
431 other aspects of the calibration methodology. Note that the calibration methodology
432 described in this document corresponds to the “last” iteration of this calibration exercise,
433 which was obtained after six iterations of the cycle mentioned on Figure 1 for the first three
434 steps of the methodology employed here. Making sure that hydrologic variables other than
435 streamflow, as well as surface variables and fluxes, are not degraded compared to the default
436 version of the model is important for two main reasons. The first reason is related to the fact
437 that the goal of this calibration exercise is to use a calibrated GEM-Hydro version in the NSRPS,
438 where various data are being assimilated to correct several variables, such as snow cover, SSM,
439 and surface temperatures. Therefore, simulation performances need at least to be maintained
440 between the default and calibrated versions of GEM-Hydro for these variables, otherwise the
441 assimilation process may be significantly altered. The second reason has to do with the
442 ultimate goal of the SVS land-surface scheme, which is to be used directly in the atmospheric
443 systems used at ECCO, with the vision of using the same systems both for Numerical Weather
444 Prediction (NWP) and hydrologic forecasts. As such, calibrating SVS to optimize streamflow
445 performances should not lead to degrading the surface temperatures and fluxes, otherwise
446 this would have a negative impact on weather forecasts.

447 Finally, it is important to emphasize that Raven and WATROUTE are two different routing
448 schemes. Therefore, even if some parameters calibrated using Raven could be directly
449 transferred into WATROUTE (such as the two parameters FLZCOEFF and PWRC related to the
450 groundwater discharge computation, see Table 1), the others could not, because some
451 processes were not represented the same way in the two routing schemes. Therefore, the
452 other WATROUTE parameters remained unchanged compared to the default version of the
453 model. Nevertheless, it was tried to further tune the WATROUTE Manning roughness
454 coefficients, by manually adjusting these values for each of the 6 subdomains with the
455 calibrated GEM-Hydro version. However, since no significant performance gain could be
456 further achieved this way, it was preferred to use the default WATROUTE values for these
457 parameters.

458 4) Modifications to the GEM-Hydro setup

459 Then, significant changes were brought to the GEM-Hydro setup using the calibrated
460 parameters (see step 4 of Figure 1), to assess the potential benefit that the calibrated
461 parameters could bring when employed with a GEM-Hydro model configuration that is close
462 to the one employed in the NSRPS system. This modified setup was the one used to produce
463 the GEM-Hydro outputs that are being shared in this dataset. More details about this “final”
464 GEM-Hydro setup are provided below. A comprehensive evaluation of the GEM-Hydro
465 performances obtained after this step was performed to make sure that no significant
466 degradation was noticed for streamflow, auxiliary hydrologic and near-surface variables (see
467 “technical validation”), when compared to the GEM-Hydro setup used in step 2. Table 3 below
468 summarizes the main modifications brought to the GEM-Hydro setup during this step.

469

470

471

472 *Table 3: Main differences between the GEM-Hydro setup used during step 2 of Figure 1 (the “GRIP-GL” setup) and*
473 *the one used during step 4 (the “NSRPS” setup). ¹: see Mai et al. (2021¹²) for more information about the geophysical*

474 *fields used during the GRIP-GL project. Precip. PPM: precipitation phase partitioning method. See text for more*
 475 *details about the NSRPS setup. See Figure 1 for the different steps of the methodology employed here.*

	Forcings	Calibrated parameters	Geophysical fields	Modelling option	Model version
GRIP-GL setup (step 2)	CaSR v2.0	Fixed for each subdomain	GRIP-GL	Precip. PPM: 0-degree threshold	GEM-Surf 6.1.2
NSRPS setup (step 4)	CaSR v2.1	Smoothed at subdomain boundaries	NSRPS	Precip. PPM: Harder and Pomeroy (2013 ³⁰)	GEM-Surf 6.2.0

476

477 **4.1- Changes to the surface component**

478 GEM-Surf version 6.2.0 was used. The different GEM-Surf options of this “final” GEM-
 479 Hydro setup are not described here in detail. We refer to the readme file of the dataset
 480 (Gaborit 2024¹³) for the list of the options used in GEM-Surf. One important change, however,
 481 is that this final setup is using the precipitation phase partitioning method (PPM) of Harder
 482 and Pomeroy (2013³⁰) whereas the previous setup used a 0°C. threshold on air temperature
 483 to split between rainfall and snowfall. Using a humidity-based PPM such as Harder and
 484 Pomeroy (2013³⁰) strongly improved the ability of GEM-Hydro to predict the precipitation
 485 phase (Vionnet et al. 2022³¹). Atmospheric forcings come from version 2.1 of the Canadian
 486 Surface Reanalysis (CaSR) (Gasset et al. 2021²⁴). Regarding the geophysical fields, the final
 487 GEM-Surf setup relies on the following data sources, which for some of them differ from the
 488 sources used during GRIP-GL (see Mai et al. 2022¹²).

489 - The Global Multi-resolution Terrain Elevation Data version 2010 (GMTED 2010, see USGS,
 490 2010³²) was used for surface topography (elevation, slope) and WATROUTE elevation data
 491 (different from the one used in GRIP-GL).

492 - The Climate-Change Initiative – Land Cover dataset version 2015 (CCI-LC 2015, see ESA,
 493 2015³³) was used for land use / land cover in GEM-Surf and WATROUTE (different from the
 494 one used in GRIP-GL).

495 - The Global Soil Dataset for Earth system modelling (GSDE, see Shangguan et al. 2014³⁴) was
 496 used for soil texture.

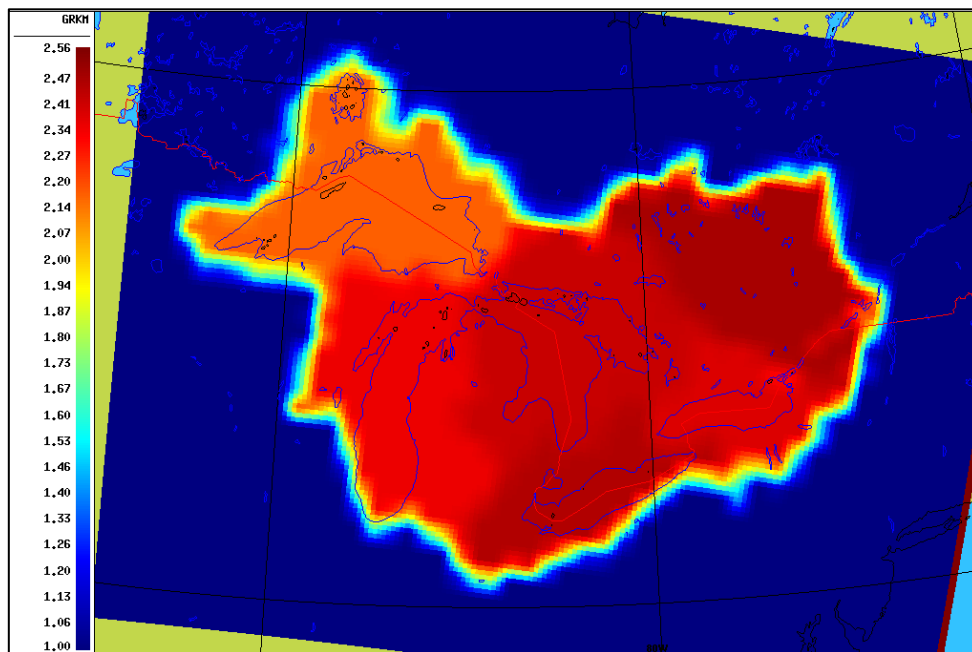
497 - The National Hydrographic Network (NHN, see Natural Resources Canada, 2020³⁵) and the
 498 National Hydrographic Dataset (NHD, see USGS, 2021³⁶) were used for drainage density.

499 - HydroSHEDS 30 arcsec. (~1km) resolution (HydroSHEDS, 2021³⁷) was used for WATROUTE
 500 flow direction grids.

501 However, in opposition to the actual NSRPS configuration, and similarly to the GEM-
 502 Hydro version used during step 2 of Figure 1 (the “GRIP-GL” configuration), subgrid-scale lakes
 503 were still deactivated during step 4. This means that when a grid cell contains less than 100%
 504 water, the water tile inside that grid-cell is not considered by the model but is replaced by the
 505 other surface tiles of the grid cell while preserving their relative importance. Grid-cells
 506 containing 100% of water were not modified as no other surface tile could replace the water
 507 tile. This “filtering” of water surfaces was also not done for grid cells located around pixels
 508 containing 100% water. This filtering is needed because with the model currently used in GEM-
 509 Hydro to represent water surfaces, an external source has to be used for water temperature
 510 and ice fraction. Generally, an ECCC internal analysis is used for that, but it is not available over
 511 the whole period of this study. Therefore, ERA-Interim was used to provide this information,

512 for consistency throughout the whole period. However, based on tests performed with this
513 source, it is not judged reliable in terms of the resulting evaporation simulated over water with
514 GEM-Hydro. Therefore, it was preferred to neglect the water portion of the grid-cells where
515 possible, leading to filtering out the subgrid-scale lakes from the GEM-Hydro setups used
516 during this study. This is why only the hydrologic variables over land are provided in this
517 dataset, and not over water surfaces (see data records). Note that neglecting the subgrid-scale
518 lakes in GEM-Hydro has a limited impact on the resulting streamflow simulations of the region,
519 based on tests previously performed (not shown here).

520 The GEM-Surf calibrated simulations were performed using a single model setup
521 covering all of the geographic region of interest (i.e., all of the 6 subdomains were included in
522 this single setup). To do so, the calibration parameters (i.e. the multiplying coefficients of Table
523 1) were provided as 2-D input fields to GEM-Surf (similarly to other static geophysical fields).
524 However, to avoid abrupt parameter changes at subdomain boundaries, the 2-D parameter
525 fields were smoothed. Not doing so could ultimately create abrupt changes in some surface
526 fluxes or variables at these boundaries, which is not desirable in the (future) context of
527 coupling this calibrated version with an atmospheric model. To smooth the calibrated
528 parameter values, the 2-D fields of the fixed parameters values for each subdomain were
529 combined and then aggregated by a factor of 3 (i.e., decreasing the resolution by a factor of
530 3), before being bilinearly interpolated back on the original grid resolution. Figure 4 shows an
531 example smoothed 2-D field for the GRKMOD calibrated parameter.



532

533 *Figure 4: example smoothed 2-D field of the GRKMOD calibrated parameter values that were provided as input to*
534 *GEM-Hydro when using a single model setup over the full Great-Lakes and Ottawa River domains. Outside of these*
535 *domains, the default (uncalibrated) value of 1.0 is applied to this parameter. See Table 1 for the definition of the*
536 *GRKMOD parameter.*

537 **4.2- changes to WATROUTE:**

538 The ECCC version 3.4 of WATROUTE was used. Similarly to the GEM-Surf component, as
539 part of the “final” GEM-Hydro open-loop run, WATROUTE was run using a single setup over
540 the full Great Lakes and Ottawa River region. To do so, the two parameters that were
541 calibrated with Raven and transferred into WATROUTE were also provided to WATROUTE as
542 2-D static fields. Note that in this case however, no smoothing of the parameter values was

543 performed at subdomain boundaries, because in the current GEM-Hydro implementation, the
544 surface and routing components of GEM-Hydro are one-way coupled, such that the routing
545 component cannot have any impact on the surface component (and therefore on the
546 atmospheric model).
547

548 5) Methods for processing the GEM-Hydro outputs:

549 **5.1- Surface variables**

550 - Fluxes: PR, ACWF, TRAF, ALAT, and O1 (in mm/h, see Data records):

551 GEM-Hydro runs over long periods by performing 24-h cycles of continuous
552 integrations, between 12:00 UTC and 12:00 UTC the day after. For each of these 24-h cycles,
553 the raw output fluxes consist of accumulated values in mm since the start of the 24-h
554 integration. These raw outputs were then processed in order to compute the "decumulated"
555 fluxes, such that each flux provided in this dataset consists of the quantity of water (in units
556 of kg/m², or mm) over the hour preceding the date mentioned. All dates of the GEM-Hydro
557 surface variables shared in this dataset correspond to time in the Universal Time Coordinated
558 (UTC) format.

559 - Snow Water Equivalent (SWE, in mm):

560 GEM-Hydro does not directly output the mean SWE over the land part of a grid-cell.
561 GEM-Hydro (SVS) does simulate two different snowpacks over the land area of a grid cell: one
562 under high vegetation, and one over bare ground/ short vegetation. The mean land SWE in a
563 grid cell was computed from the raw outputs using Equation 4 below:

$$564 \text{SWE} = (\text{SNDP} * \text{SNDN} * 0.01 + \text{WSN}) * (1 - \text{VEGH}) + (\text{SVDP} * \text{SVDN} * 0.01 + \\ 565 \text{WSV}) * \text{VEGH} \quad \text{Eq. 4, where:}$$

566 SNDP, SVDP: snowpack depth (cm) respectively over bare ground + short vegetation, and
567 under high vegetation.

568 SNDN, SVDN: snowpack density (kg/m³) respectively over bare ground + short vegetation, and
569 under high vegetation.

570 WSN, WSV: liquid water stored in the snowpack (mm), respectively over bare ground + short
571 vegetation, and under high vegetation.

572 VEGH: fraction of the land area of the grid cell that is covered with high vegetation.

573

574 - Water stored in/on vegetation (WVEG, in mm):

575

576 In SVS, the quantity of water stored in/on vegetation is valid for the fraction of the
577 land surface for which vegetation is above the snowpack. Therefore, the raw WVEG SVS output
578 was modified according to Equation 5 below, such that it corresponds to a height of water (in
579 mm) valid over the whole land surface area, in order to be used directly in Equations 6 and 7
580 to compute the SVS water balance over the land-surface area of a grid-cell (see Data Records).

581

$$582 \text{WVEG} = \text{WVEG}_{raw} * (1 - \text{PSGL}) \quad \text{Equation 5, where:}$$

583 WVEG: final WVEG variable shared in this dataset, and valid over the whole land surface area
584 of a grid-cell (in mm)

585 *WVEG_{raw}*: raw SVS output corresponding to the quantity of water (in mm) stored in the
586 vegetation fraction of a grid-cell's land tile that is above the snowpack.

587 *PSGL*: fraction of the land surface that is covered with snow over bare ground and snow over
588 low vegetation.

589 - Soil moisture (WSL1-6, m³/m³):

590 No manipulation of the raw soil moisture outputs was performed but information is
591 provided here on how to convert the values provided in this dataset. Soil moisture has units
592 of m³/m³: it represents the fraction of a given soil layer that is filled with liquid water (the
593 version of SVS used here does not represent freeze/thaw processes). In order to convert soil
594 moisture from m³/m³ into soil moisture with units of mm (needed to compute the SVS water
595 balance for example, see Equations 6 and 7), one needs to multiply the soil moisture (m³/m³)
596 for a given soil layer by the thickness of this soil layer in mm. Then, one could sum up the soil
597 moisture content over the six soil layers in mm to obtain the total amount of water stored in
598 the SVS soil column, in units of mm. The depth of the SVS soil layers are mentioned in Table 4,
599 but their thickness is mentioned below in mm. The total soil thickness in this GEM-Hydro
600 configuration is equal to 2000mm (2m).

601 - soil layer 1: depth between 0 and 5 cm, thickness of 50mm

602 - soil layer 2: depth between 5 and 10 cm, thickness of 50mm

603 - soil layer 3: depth between 10 and 20 cm, thickness of 100mm

604 - soil layer 4: depth between 20 and 40 cm, thickness of 200mm

605 - soil layer 5: for depth between 40 and 100 cm, thickness of 600mm

606 - soil layer 6: for depth between 100 and 200 cm, thickness of 1000mm

607

608 For all of the GEM-Surf outputs (2D gridded fields, so all except streamflow) provided
609 in this dataset (except the WT variable), the fields were then filtered in order to remove the
610 values located outside of the region of interest, i.e. outside of each of the five Great-Lakes
611 watersheds, and outside of the Ottawa River watershed. This was done because the calibrated
612 parameter values only apply inside of these watersheds. Therefore, outside of them, the GEM-
613 Hydro outputs correspond to the default version of the model. It was preferred not to mix
614 outputs corresponding to the default version of the model with outputs corresponding to the
615 calibrated version of the model in the same files included in this dataset. The values filtered
616 out were replaced by "NaN" values. However, the WT variable is not simulated by the model
617 and corresponds to a static field that represents the fraction of the grid-cell occupied by land
618 in the setup used here. It is reminded that subgrid-scale lakes were deactivated here (see point
619 4.1) such that most of the grid cells outside of the big lakes have a WT value (land fraction)
620 equal to 1.0 here (100% land). Therefore, this field was not filtered out outside of the region
621 of interest.

622 For all of the GEM-Surf outputs (2D gridded fields, so all except streamflow), the
623 standard files (a binary format used internally at ECCC) were all converted into the netcdf
624 format. All dates associated with the GEM-Surf variables shared in this dataset correspond to
625 time in the Universal Time Coordinated (UTC) format.

626 **5.2- Streamflow:**

627 The WATROUTE component of GEM-Hydro produces streamflow at a 1-km resolution,
628 with an hourly time-step. However, in this dataset, we only provided simulated and observed
629 streamflow time-series for the grid cells containing a flow gauge. Moreover, the hourly flows
630 were converted into mean daily flows because a daily time-step was used to evaluate model

631 performances regarding streamflow. The daily flows shared in this dataset for a given date are
632 valid between 00:00 and 00:00 the day after in local time, i.e. from midnight to midnight, with
633 time always corresponding to the Eastern Daylight Time (EDT, corresponding to UTC minus 4
634 hours). More information on the 212 flow gauges for which mean daily flows are reported in
635 this dataset can be found in Mai et al (2022¹²), or on the USGS and Water Survey of Canada
636 (WSC) websites mentioned below. The United States' (US) streamflow observations included
637 in this dataset come from the US Geological Survey (USGS) website mentioned below.

638 https://waterdata.usgs.gov/nwis/dv/?referred_module=sw (accessed on December 1st, 2023)

639 https://wateroffice.ec.gc.ca/search/historical_e.html (accessed on December 1st, 2023)

640 The Canadian daily streamflow observations were obtained from the HYDAT database
641 available for download here:

642 [National Water Data Archive: HYDAT - Canada.ca](https://waterdata.usgs.gov/nwis/dv/?referred_module=sw) (accessed on December 1st, 2023).

643

644 Data Records

645

646 The GEM-Hydro model hydrologic outputs shared in this dataset (Gaborit 2024¹³) were
647 published on the Federated Research Data Repository (FRDR) and cover the period from 2001-
648 01-01 to 2018-12-31. The outputs are available over the Canadian/USA watersheds of the
649 Great Lakes, and over the Ottawa River watershed. In other words, they are available over the
650 watersheds of Lake Superior, Lake Michigan, Lake Huron and Georgian Bay watershed, Lake
651 Erie and Lake Saint-Clair watershed, Lake Ontario watershed, and the Ottawa River watershed
652 (Canada, provinces of Ontario/Québec). These outputs consist of all variables (hourly fluxes
653 and state variables) related to the water balance (see Equations 6 and 7 below) of the land-
654 surface tile (SVS) of the surface component of GEM-Hydro (GEM-Surf), and of the mean daily
655 streamflow time-series (observed and simulated with the WATROUTE routing component of
656 GEM-Hydro), at the 212 gauge locations of the region of interest.

657 The equations of GEM-Hydro land-surface (SVS) water balance can be written as follows for
658 any grid-cell and over any temporal period:

659 $\Delta S = PR - (ACWF + TRAF + ALAT + O1)$ Equation 6), with:

660 ΔS : Change in storage (final storage – initial storage) between the final and initial dates of the
661 period being considered, in mm (or kg/m²).

662 $PR, ACWF, TRAF, ALAT, O1$: Accumulated values of the different SVS water fluxes (see Table
663 4) over the period being considered, in mm or kg/m².

664 The equation to compute the SVS water storage for any given date is given below:

665 $S = WVEG + SWE + \sum_{i=1,6}(WSL_i * H_i)$ Equation 7), where:

666 S : Total water stored in the SVS land-surface scheme for a given date, in mm or kg/m².

667 $WVEG, SWE, WSL_x$: The three different SVS variables related to water storage (see Table 4),
668 in mm or kg/m².

669 H_i : Thickness of the i^{th} SVS soil layer, in mm (see Table 4).

670

671 For the gridded surface variables (i.e. all except streamflow), the grid has a 0.09 degree
672 resolution (~10km) and a size of 191x143 grid cells, but the values are not provided outside of
673 the aforementioned watersheds (see point 5.1 in “Methods”). Moreover, these gridded
674 variables are all valid over the land fraction of a grid cell only, and not over other surface types
675 like water. In other words, these variables correspond to outputs of the GEM-Hydro land-

676 surface scheme SVS. Therefore, over pixels that are covered with 100% water in the domain,
677 all of the gridded surface variables of this dataset have a value of 0.0, except soil moisture
678 which has a value of 1.0 for these water pixels, for aesthetic purposes. However, note that the
679 subgrid-scale lakes were removed from the GEM-Hydro setup (see point 4.1 of “Methods”),
680 meaning that most of the grid cells of the region are assumed to be occupied at 100% by land
681 cover in GEM-Hydro, except around grid cells and in grid cells that are occupied by 100% water
682 (see the field WT mentioned below). In any case, the gridded surface variables of this dataset
683 can still be used as-is, for example to drive a routing model over the region (see Usage Notes).
684 More information about the reason for (and the impact of) neglecting the subgrid-scale lakes
685 in the GEM-Hydro setup used here can be found in point 4.1 of the “Methods” section. The
686 land cover fraction inside each grid cell does not evolve with time in this version of GEM-Hydro
687 and is provided in this dataset as the “WT” variable.

688 The SM values shared in this dataset (see Table 4) correspond to liquid water only,
689 because the version of SVS used during this study does not include the representation of soil
690 freeze/thaw processes, and therefore does not simulate the conversion from liquid to frozen
691 soil water, during cold seasons. This is because when activating the soil freeze-thaw processes
692 with SVS, spring freshets are generally strongly overestimated, partly because the model does
693 not allow for infiltration into frozen ground, which could occur in reality because of
694 macropores (Mohammed et al., 2018³⁸). Work is under way to improve the representation of
695 the soil freeze-thaw processes with SVS, and their impact on resulting streamflow simulations.

696 Table 4 summarizes the different files shared in this dataset, as well as their content.
697 Note that each file of this dataset contains a unique hydrologic variable, over the region of
698 interest and over the full period of interest, except for streamflow, where the file shared is a
699 compressed file. Once unzipped, there will be one text file for each of the 212 flow gauges
700 considered in the domain, containing the daily observed and simulated streamflow over the
701 full period.

702

703
704
705

Table 4: list of files shared in this dataset and description of their content. See point 5.1 in “Methods” for more details about the computations performed with the actual GEM-Hydro outputs to produce the variables mentioned in this table.

Filename (Hydrologic variable)	Hydrologic Variable	Units	Definition
GEM-Hydro_calibrated_PR.nc	PR	mm/h	Hourly total precipitation over the hour preceding the date mentioned
GEM-Hydro_calibrated_ACWF.nc	ACWF	mm/h	Hourly evapo-transpiration over land surface over the hour preceding the date mentioned
GEM-Hydro_calibrated_TRAF.nc	TRAF	mm/h	Hourly surface runoff over land surface over the hour preceding the date mentioned
GEM-Hydro_calibrated_ALAT.nc	ALAT	mm/h	Hourly total lateral flow from land surface soil column (from all active soil layers) over the hour preceding the date mentioned
GEM-Hydro_calibrated_O1.nc	O1	mm/h	Hourly drainage from (vertical water flux leaving the) land surface last active soil layer over the hour preceding the date mentioned
GEM-Hydro_calibrated_WVEG.nc	WVEG	kg/m ² or mm	Water stored in/on the land surface vegetation at the date mentioned, but weighted such that it corresponds to an average height of water valid over the whole land surface
GEM-Hydro_calibrated_SWE.nc	SWE	kg/m ² or mm	Average Snow Water Equivalent over land surface at the date mentioned
GEM-Hydro_calibrated_WSL1.nc	WSL1	m ³ /m ³	Soil moisture content for soil layer 1: for depth between 0 and 5 cm (volumetric fraction) at the date mentioned
GEM-Hydro_calibrated_WSL2.nc	WSL2	m ³ /m ³	Soil moisture content for soil layer 2: for depth between 5 and 10 cm (volumetric fraction) at the date mentioned
GEM-Hydro_calibrated_WSL3.nc	WSL3	m ³ /m ³	Soil moisture content for soil layer 3: for depth between 10 and 20 cm (volumetric fraction) at the date mentioned
GEM-Hydro_calibrated_WSL4.nc	WSL4	m ³ /m ³	Soil moisture content for soil layer 4: for depth between 20 and 40 cm (volumetric fraction) at the date mentioned
GEM-Hydro_calibrated_WSL5.nc	WSL5	m ³ /m ³	Soil moisture content for soil layer 5: for depth between 40 and 100 cm (volumetric fraction) at the date mentioned
GEM-Hydro_calibrated_WSL6.nc	WSL6	m ³ /m ³	Soil moisture content for soil layer 6: for depth between 100 and 200 cm (volumetric fraction) at the date mentioned
GEM-Hydro_calibrated_WT.nc	WT	[-]	Fraction of grid cell occupied by land surface (constant over time).
GEM-Hydro_calibrated_streamflow.zip	Q	m ³ /s	Pairs of observed and simulated mean daily streamflow at flow gauge locations in txt format. Once unzipped, one file per gauge. The .txt filenames correspond to a US or Canadian gauge ID.

706
707
708

Technical Validation

A) Streamflow performances

709
710
711
712
713
714
715
716
717
718
719
720
721
722
723
724
725
726
727

To perform the evaluation of GEM-Hydro streamflow simulations over the Great-Lakes and Ottawa river basins, the mean daily GEM-Hydro simulated streamflows were computed at the location of the 212 streamflow gauges used in the GRIP-GL project (Mai et al. 2022¹²), for which mean observed daily streamflow is available, over the period from January 1st 2001 to December 31st, 2017. Despite the GEM-Hydro simulations performed here also cover the year 2018, it was not considered in this evaluation, because the observations were gathered from the data of the GRIP-GL project, which does not include the year 2018. For a description of the flow gauges main attributes (gauge ID, river name, drainage area, mean elevation and mean annual runoff, etc.), please refer to the supplementary material of GRIP-GL (Mai et al. 2022¹²). The subbasins corresponding to these 212 flow gauges are shown on Figure 2. Figures 5 and 6 show boxplots of streamflow performances across these 212 flow gauges, either over the calibration (2008/01/01-2017/12/31) or validation period (2001/01/01-2007/12/31), for MESH-SVS-Raven and different versions of GEM-Hydro, and for three different scores. The scores include the revised KGE criteria (see Kling et al. 2012²⁸), the Nash-Sutcliffe criteria (NSE, see Nash and Sutcliffe, 1970³⁹) and a relative percent bias criteria (see Equation 8 below).

728
$$PBIAS = \frac{\sum_{i=1}^N (O_i - S_i)}{\sum_{i=1}^N O_i} * 100 \quad \text{Eq. 8, where:}$$

729 $PBIAS$: Relative Bias in percent

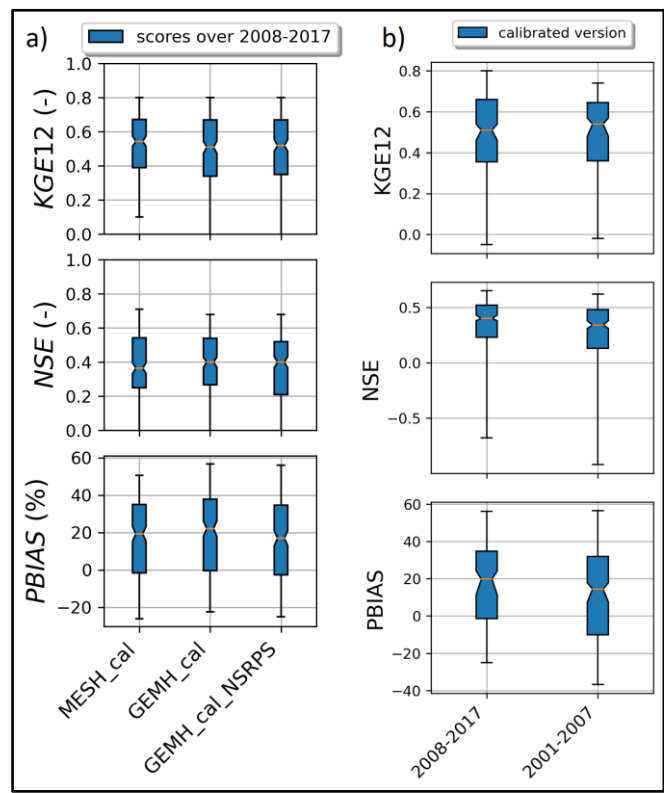
730 O_i : Observed streamflow for day i

731 S_i : Simulated streamflow for day i

732 Therefore, when the $PBIAS$ value is positive (negative), it denotes an underestimation
 733 (overestimation) of the observed flows by the simulations.

734 First, it can be seen on Figure 5a that when the SVS and some routing parameters are
 735 calibrated with MESH-SVS-Raven and then transferred into GEM-Hydro, the streamflow
 736 performances remain relatively similar, highlighting the relevance of the approach used here
 737 to calibrate SVS and some routing parameters using another system than GEM-Hydro. The
 738 same is true when modifications are made to the GEM-Hydro setup in order to use a
 739 configuration that is more representative of the one used in the NSRPS system. This is
 740 encouraging because it supports the idea that the calibrated parameters obtained here with
 741 MESH-SVS-Raven were not overfitted to the specific setup configuration used with MESH-SVS-
 742 Raven and can actually be transferred to a GEM-Hydro version using a different setup
 743 configuration. The absence of over-calibration or overfitting in the calibrated parameter
 744 values obtained here is moreover supported by the evaluation of the auxiliary hydrologic and
 745 near-surface variables presented further down.

746
 747

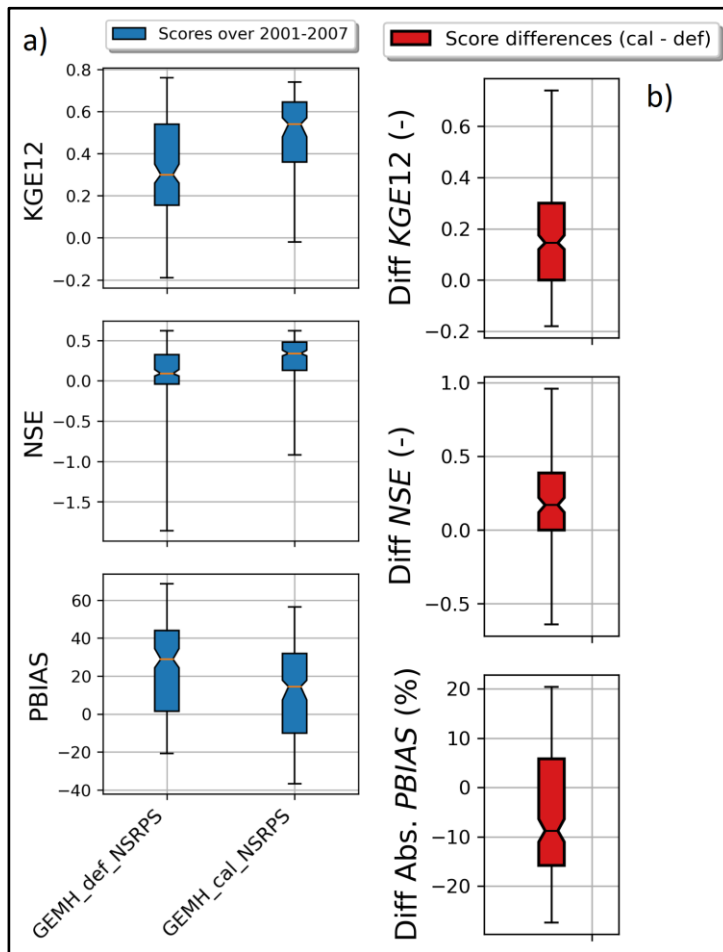


748

749 *Figure 5: Boxplots of streamflow performances across the 212 flow gauges considered here, for the*
 750 *different calibrated models. a) performances over the calibration period (1st Jan. 2008- 31 Dec. 2017) for the three*
 751 *different calibrated model runs mentioned in this document. MESH_cal corresponds to the calibrated version of*
 752 *MESH-SVS-Raven using the GRIP-GL setup configuration, GEMH_cal corresponds to the calibrated version of GEM-*
 753 *Hydro using the GRIP-GL setup configuration, and GEMH_cal_NSRRPS corresponds to the calibrated version of GEM-*
 754 *Hydro using the NSRPS setup configuration (see Methods and text for more details). b) performances for the*
 755 *calibrated version of GEM-Hydro using the NSRPS configuration over the calibration (20080101-20171231) and*
 756 *validation (20010101-20071231) periods. The target value for KGE12 (revised KGE) and NSE criteria is 1.0, while the*

757 *target value for PBIAS (relative percent bias) is 0.0. On figures 5 and 6, the lower and upper limits of the boxes*
758 *correspond respectively to quartiles 25 and 75% of the 212 gauges' performances, the median score value is shown*
759 *with a horizontal line in the thinner part of the box, and the lower and upper whiskers correspond respectively to*
760 *percentiles 5 and 95% of the gauges' performances, while the outliers are not shown.*

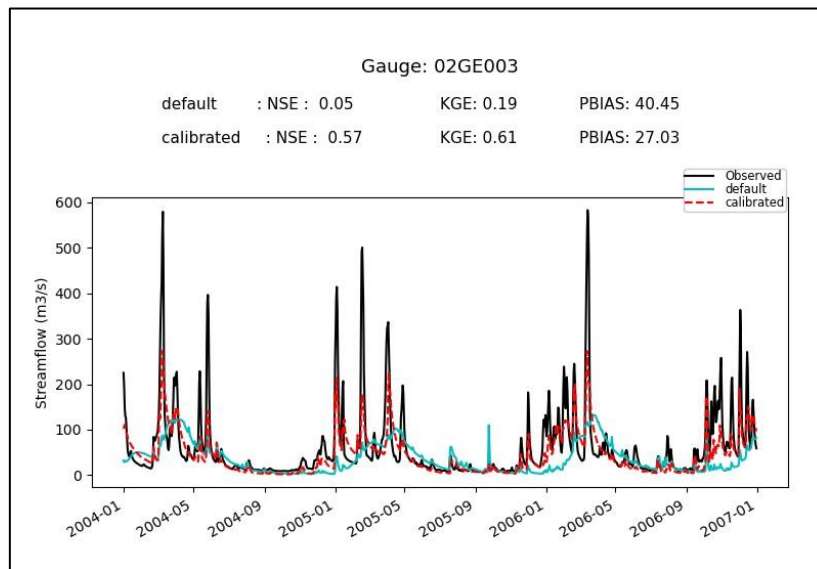
761 It can be seen on Figure 5b that the calibrated version of GEM-Hydro displays a strong
762 temporal robustness, because the streamflow performances are generally similar between the
763 calibration and validation periods. Finally, it can be seen on Figure 6 that the calibrated version
764 of GEM-Hydro generally displays better streamflow performances than the default version of
765 the model (without calibration), with a median KGE improvement close to 0.2 (see Figure 6b).
766 It can also be seen on Figure 6b that regarding the KGE and NSE criteria, an improvement
767 occurred for 75% of the 212 flow gauges considered. However, it also means that for 25% of
768 the stations, the calibrated version of GEM-Hydro actually degrades flow performances
769 compared to the default version of the model. When looking at flow hydrographs, this was
770 generally attributed to overestimated streamflow peaks and flow volumes. This is supposed
771 to be caused by the calibrated parameters obtained here, which imply a significant increase in
772 the horizontal and vertical hydraulic conductivities in agricultural areas, especially for the
773 watersheds of Lake Erie and Lake Ontario. This is because GEM-Hydro is missing an explicit
774 representation of the tile drains in these areas, and because of the strategy employed here to
775 represent the effect of these tile drains in the model (see Methods). Indeed, with this strategy,
776 tile drains are assumed to be present in 100% of the agricultural areas, which is probably not
777 the case in reality. Therefore, where tile drains are present in reality, the calibration
778 methodology employed here generally leads to an improvement of the simulations compared
779 to the default version of the model (but still to generally underestimated flow volumes, see
780 for example Figure 7), while when tile drains may not be present in reality, the calibrated
781 parameters lead to overestimated flows (see Figure 8). Therefore, the final calibrated values
782 for GRKMO_A and KASMO_A (see Figure 3) consist of a trade-off between agricultural areas
783 that are strongly impacted by human influence, and those that are less influenced. This may
784 be improved in the future for example by using a GRKMO_A calibration parameter that would
785 only be tied to areas where tile drains are actually present, and a KASMO_A calibration
786 parameter only tied to areas where significant ploughing practices occur, instead of being
787 applied to all agricultural areas. However, this information would need to be available on maps
788 (over the US and Canada), which was not the case at the time of this study, to the extent of
789 our knowledge. This is therefore dedicated to future work. For the time being, we consider
790 that the calibrated version of GEM-Hydro, whose outputs are described here, generally
791 represents an improvement upon its default counterpart, for most of the Great-Lakes and
792 Ottawa River watersheds.
793



794
795

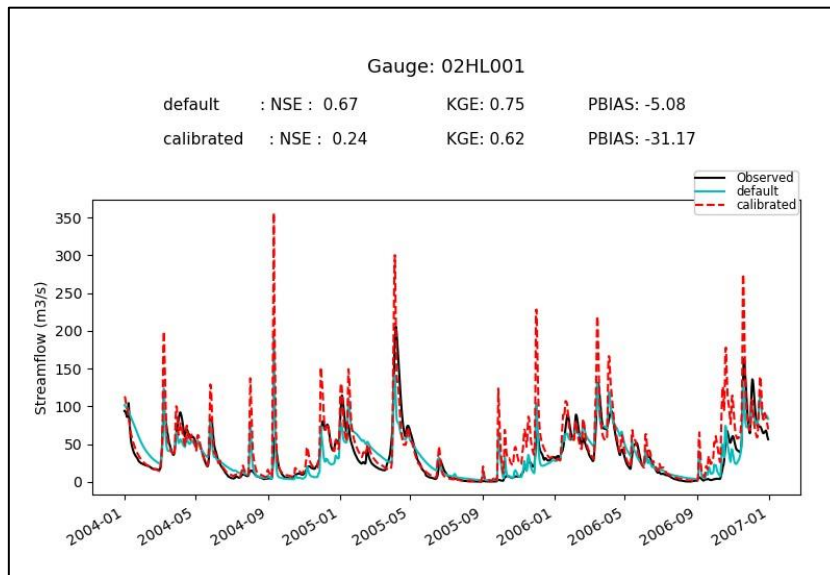
796 *Figure 6: boxplots of streamflow performances across the 212 flow gauges considered here, for the default and*
 797 *calibrated versions of GEM-Hydro over the validation period (20010101-20071231), and using the NSRPS*
 798 *configuration. a) Performances of each version separately. GEMH_def_NSRPS corresponds to the default GEM-*
 799 *Hydro version. GEMH_cal_NSRPS corresponds to the calibrated version of GEM-Hydro. b) Differences in streamflow*
 800 *performances between the two versions of GEM-Hydro. For the KGE and NSE criteria, the difference between the*
 801 *calibrated and default versions of GEM-Hydro was computed at each gauge location, and values above 0.0 indicate*
 802 *an improvement of the calibrated upon the default version of the model. For the PBIAS criteria, the difference*
 803 *between the calibrated and default version of the model was computed using the absolute PBIAS value of each*
 804 *version and at each gauge location, and negative values indicate an improvement of the calibrated upon the default*
 805 *version of the model. See legend of Figure 5 for more details on the scores and the boxplots shown here.*

806
807



808
809
810
811
812

Figure 7: Hydrographs for gauge 02GE003, for the default and calibrated versions of GEM-Hydro, over a three-year period of the validation period. A three-year period is used here to better display the change in flow dynamics between the two versions. The flow observations are shown with the black line. The station 02GE003 is located on the northern shore of Lake Erie, in an agricultural area, and has a drainage area of 4498 km².



813
814
815
816
817

Figure 8: Hydrographs for gauge 02HL001, and for the default and calibrated versions of GEM-Hydro, over a three-year period of the validation period. A three-year period is used here to better display the change in flow dynamics between the two versions. The flow observations are shown with the black line. The station 02HL001 is located on the northern shore of Lake Ontario, in an agricultural area, and has a drainage area of 2673 km².

818
819
820

B) GEM-Hydro auxiliary hydrologic variables

821
822
823
824
825
826
827
828
829

In order to evaluate the performances of the calibrated version of GEM-Hydro beyond streamflow performances, the default and calibrated versions of GEM-Hydro (using the final NSRPS configuration) were compared with regard to the performances of auxiliary hydrologic variables, as was done in GRIP-GL (Mai et al. 2022¹²), but also from the view point of near-surface meteorological variables (see point C below). This is important to evaluate a physically-based model with other variables than streamflow, especially in the case where the model was calibrated to maximize only streamflow performances, in order to make sure that the calibration process did not result in degrading other physical processes in the model (Kirchner 2006⁴⁰). This can often happen during calibration, that the final performances are good with

830 regard to streamflow but imply unrealistic physical processes. This is in opposition to the idea
 831 of “getting the right answer for the right reasons” (Kirchner 2006⁴⁰). Getting the right answer
 832 for wrong reasons is linked with the notion of parameter equifinality (Beven and Binley
 833 1992⁴¹): very different parameter sets, all leading to similar streamflow performances, can
 834 imply very different internal physical processes, some of which may be unrealistic to various
 835 degrees. This is especially important to assess the performances of the calibrated SVS version
 836 for other variables, in the context where this land-surface scheme could ultimately be two-
 837 way coupled with an atmospheric model, as mentioned in the “Methods” section.

838 Therefore, the goal here is to make sure that the performances of the calibrated
 839 version of GEM-Hydro remain similar or are better than the default version of the model, when
 840 looking at other outputs of the model. Here we focus on three hydrologic variables other than
 841 streamflow: the model total ET over land (which in GEM-Hydro is the sum of bare ground
 842 evaporation and vegetation ET, in mm), the SSM (mean soil moisture between 0 and 10cm
 843 depth, in m³/m³), and the mean SWE on the ground (in mm). In order to evaluate these
 844 variables, their mean daily value was computed from the hourly GEM-hydro outputs (or the
 845 total value in the case of AET), and compared to a reference dataset for each of them. The
 846 total AET over land is a direct output of GEM-Hydro that is being shared in this dataset, the
 847 mean SVS SWE was computed as specified in the Data Records section, and the SSM between
 848 0 and 10cm was simply computed by taking the average of soil moisture for the first two SVS
 849 soil layers.

850 The reference datasets are mentioned in Table 5. They are the same as those used
 851 during GRIP-GL (Mai et al. 2022¹²). Note that these datasets do not consist of purely observed
 852 data, and as such, they cannot be considered as the “truth” for these variables. However, the
 853 idea here is not to perform a comprehensive evaluation of the calibrated version of GEM-
 854 Hydro, but rather to compare it to the default version of the model to make sure that the
 855 performances remain at least similar between the two. Note that regarding ERA-5 Land that
 856 is used as the reference for the SWE, it was preferred upon in-situ measurements of SWE
 857 because in-situ SWE measurements are not gridded (they are not available for all pixels of the
 858 region), and are not available on a daily basis either. However, an evaluation of the calibrated
 859 GEM-Hydro version and ERA-5 Land against in-situ SWE measurements is also performed here.

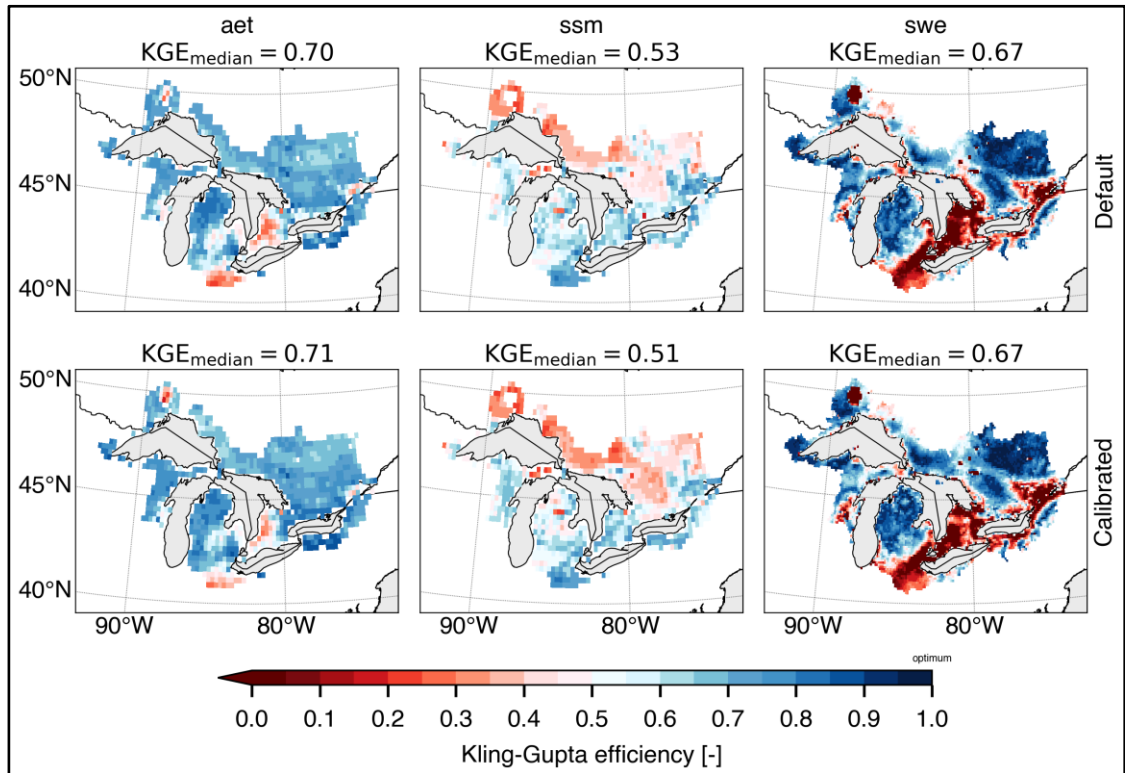
860
 861

Table 5: List of the reference datasets used to evaluate the GEM-Hydro auxiliary hydrologic variables.

Variable	Reference dataset
Evapo-transpiration, in mm	GLEAM v3.5b: GLEAM Global Land Evaporation Amsterdam Model See also Martens et al. (2017⁴⁴)
Soil moisture (0-10cm), in m ³ /m ³	GLEAM v3.5b: GLEAM Global Land Evaporation Amsterdam Model See also Martens et al. (2017⁴⁴)
SWE (mm)	ERA-5 Land See product documentation and Muñoz Sabater (2019⁴⁵)

862
 863

864 The evaluation against these reference datasets was performed by computing the KGE
 865 criteria for each grid cell of the full domain, using the time-series of mean daily (or total daily
 866 for AET) values of these variables. Note that in this case, the KGE values correspond to the
 867 original (not revised) formulation of the KGE, as proposed by Gupta et al. (2009⁴²). For AET and
 868 SSM, the period from 2003 to 2017 was used because this is the period for which the GLEAM
 869 v3.5 data were available, but for the comparison against ERA-5 Land regarding SWE, we used
 870 the period from 2001 to 2017. Finally, the GEM-Hydro outputs were re-gridded to the
 871 resolution of the reference datasets, which is of 0.25° for the GLEAM dataset (AET and SSM),
 872 and of 0.1° for ERA-5 Land (SWE). See Mai et al. (2022¹²) for more details on the auxiliary
 873 variables' evaluation.
 874



875
 876 *Figure 9: Comparison of the two versions of GEM-Hydro against reference datasets for the auxiliary hydrologic*
 877 *variables. The top row shows the comparison for the default GEM-Hydro version, while the comparison of the*
 878 *calibrated version is shown on the bottom row). The three auxiliary hydrologic variables considered here consist of*
 879 *evapo-transpiration (aet, left column), superficial soil moisture (ssm, middle column), and snow water equivalent*
 880 *(swe, right column).*

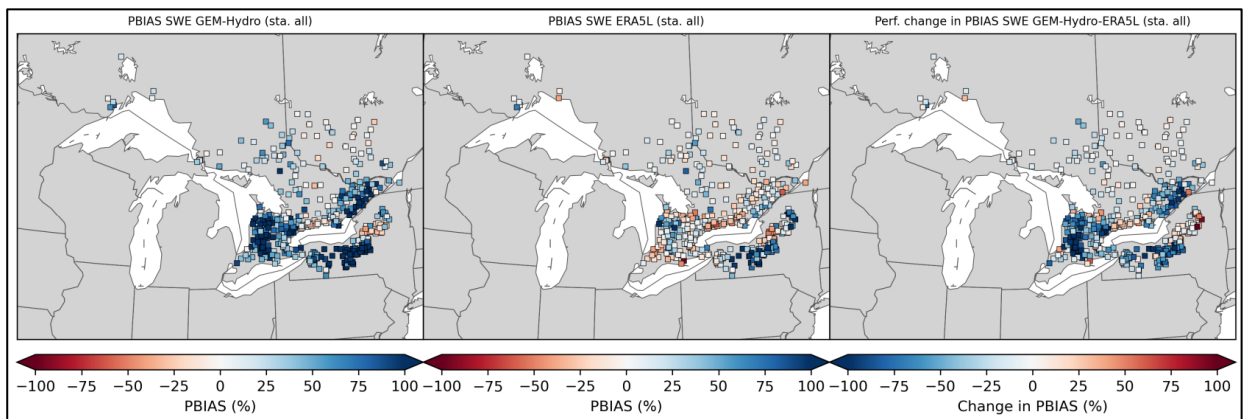
881 It can be noticed on Figure 9 that the default and calibrated versions of GEM-Hydro
 882 generally display similar performances when compared to the reference datasets used here.
 883 Note that to achieve these results, a total of 6 full calibration trials were performed (see
 884 Methods), and several modifications to the calibration methodology were applied after each
 885 iteration because for the former trials, a degradation was sometimes noticed with the
 886 calibrated version of GEM-Hydro, for some of these auxiliary variables and in some regions. As
 887 previously mentioned, this is because of the equifinality issue, that especially arises when only
 888 calibrating a physical model to streamflow. However, note that performing multi-objective
 889 calibration to include for example these three auxiliary variables in the objective function
 890 during calibration is, on one hand, not a trivial task that can itself call for several iterations of
 891 the procedure (see Mai 2023⁷), and on the second hand, a methodology that could lead to
 892 suboptimal streamflow performances (Mei et al. 2023⁹). However, maximizing streamflow
 893 performances was the main objective of the calibration work performed here, in order to
 894 ultimately improve the NSRPS real-time streamflow forecasts performed at ECCC. This is why

895 it was preferred to only target flow performances during calibration but evaluate the model
896 based on other variables afterwards.

897 It can be noticed on Figure 9 that for each of the three GEM-Hydro auxiliary variables,
898 there are some areas that display a stronger discrepancy against the reference data used here.
899 For example, for AET, the areas with stronger discrepancy consist of the northern shore of
900 Lake Erie, and the southern west portion of Lake Erie. In these areas, both GEM-Hydro versions
901 tend to overestimate AET, which was diagnosed by looking at the bias component of the KGE
902 (not shown here). Despite the exact source of this overestimation is not known, it was noticed
903 that a better match between the calibrated GEM-Hydro version and the reference dataset was
904 obtained in these areas for AET when using much higher values (close to 100.0) for the
905 KASMO_A parameter (see Table 1), but to the detriment of SSM performances, however. Since
906 it was not sure that this model response was due to the right reasons, a maximum value of 5.0
907 for KASMO_A was preferred (Table 1), leading to the results shown on Figure 9. Another issue
908 in these areas is that the SVS model currently does not represent irrigation, which may have a
909 strong effect on SSM.

910 Regarding SSM, the areas with the strongest discrepancies between GEM-Hydro and the
911 reference dataset consist of the northern part of the Great-Lakes region. Again, while the
912 reason is not exactly known, it has to be emphasized that these areas correspond to regions
913 with a high fraction of high vegetation covers, where the remotely sensed satellite soil
914 moisture data (that GLEAM assimilates) are known to be less accurate (Tong et al. 2020⁴³).
915 Therefore, it is not sure that GEM-Hydro actually performs worst in this northern region,
916 with regard to SSM. It is also emphasized that the actual KGE performances are displayed here for
917 SSM, while in the GRIP-GL project, only the correlation component of the KGE was shown for
918 this variable, given that many models were not simulating the actual soil moisture variable, or
919 not for the same depth. However, it is much easier to achieve satisfactory SSM simulations
920 with regard to correlation only, rather than for the actual KGE value that is used here. Finally,
921 regarding SWE, there are several areas showing a strong discrepancy between GEM-Hydro and
922 ERA-5 Land.

923



924
925 *Figure 10: Comparison between the bias of SWE simulations from GEM-Hydro and from ERA-5 Land, over the*
926 *watersheds considered in this study and over the period from October 1st 2001 to October 1st 2018 (17 winters). The*
927 *observations mainly consist of in-situ manual snow surveys included in the CanSWE database (Vionnet et al. 2021⁴⁶)*
928 *and taken from the northeastern US databases (Mortimer et al., 2022⁴⁷). Only stations with at least 20 observations*
929 *(~one average per winter) available were considered. For the left (GEM-Hydro bias) and middle (ERA-5 Land bias)*
930 *panels, the bias shown consists of the relative bias expressed in % (see Equation 8), but using the difference between*
931 *the simulated and observed values, in opposition to Equation 8 (see text for more details). Blue (red) colors imply*
932 *an over- (under-)estimation of the observed values. The differences between the absolute PBIAS values of ERA-5*
933 *Land and GEM-Hydro are shown on the right panel, such that red (blue) colors indicate that GEM-Hydro SWE*
934 *simulations have less (more) bias than those of ERA-5 Land.*

935

936 For the areas exhibiting strong differences between ERA-5 Land and GEM-Hydro in terms
 937 of SWE simulations (see Figure 9), it can be seen on Figure 10 that ERA-5 Land is generally
 938 better than GEM-Hydro. The strong positive *PBIAS* values observed for GEM-Hydro SWE
 939 simulations in some areas of Figure 10 correspond well to the areas for which strong
 940 differences were noticed between GEM-Hydro and ERA-5 Land, in terms of SWE (see Figure
 941 9). This SWE overestimation by GEM-Hydro (see legend of Figure 10) in these areas was less
 942 pronounced (but still present) when using the traditional 0°-threshold method to separate
 943 liquid and solid precipitation in GEM-Hydro (not shown), instead of the Harder and Pomeroy
 944 (2013³⁰) method used here for precipitation-phase partitioning (see Methods). However, the
 945 evaluation of the 0°-threshold method has shown that it creates a strong underestimation of
 946 snowfall occurrence, for many regions of Canada (see for example Vionnet et al. 2022³¹). On
 947 the other hand, evaluation of the precipitation-phase partitioning method from Harder and
 948 Pomeroy (2013³⁰) over the Great Lakes has shown that it can lead to an overestimation of
 949 snowfall occurrence (not shown here). Therefore, it is supposed that the positive bias noticed
 950 here with GEM-Hydro with regard to SWE for some areas, results from a combined positive
 951 bias in CaSR v2.1 winter precipitation forcings (Gasset et al. 2021²⁴) and a positive bias in
 952 snowfall occurrence from Harder and Pomeroy (2013³⁰). Additional investigations are required
 953 in the context of the preparation of the CaSR v3.0 and are beyond the scope of this document.
 954 However, there are areas for which the GEM-Hydro simulations performed here are very
 955 competitive with (or very close to) ERA-5 Land with regard to SWE simulations (see Figures 9
 956 and 10).

957 **C) GEM-Hydro near-surface meteorological variables**

958 As explained in the “Methods” section, it is also important to make sure that the calibrated
 959 version of GEM-Hydro does not degrade the near-surface variables simulated by the model,
 960 as compared to the default version. This is related to the fact that ultimately, the calibrated
 961 version of the surface component of GEM-Hydro could be two-way coupled with ECCC
 962 atmospheric models. The three surface variables considered here consist of 2-m air
 963 temperature (TT, in °C.), 2-m dew point (TD, in °C.), and 10-m wind speed (UV, in m.s⁻¹). It is
 964 possible to evaluate these GEM-Hydro variables because they are simulated by the model and
 965 do not consist of forcing variables. Indeed, GEM-Hydro is driven with atmospheric forcings
 966 (like air temperature and humidity and wind) corresponding to the lowest prognostic level of
 967 an atmospheric model, which in the case of the CaSR v2.1, corresponds approximately to 40
 968 m. In order to perform the evaluation of the default and calibrated versions of GEM-Hydro
 969 with regard to these variables, the ECCC internal verification tool “EMET” was used. The
 970 evaluation was performed by considering in-situ observations from the METAR, SYNOP, and
 971 SWOB observation networks over the full domain considered here, using the hourly GEM-
 972 Hydro outputs, and over the period from 2013 to 2017 included. Each one of the two GEM-
 973 Hydro versions was evaluated by computing the mean bias and the standard deviation of the
 974 error of the simulations, as compared to the observed values of a given variable, over a given
 975 period. The average of a given score was then computed over the area of interest. Then, the
 976 performances of the two versions were compared and are shown in Table 5, which shows the
 977 relative differences between the performances of the two versions of GEM-Hydro (i.e., default
 978 and calibrated).

981
 982 To compute the relative bias differences, Equation 9 below was used:

983
$$REL.\Delta BIAS = \frac{|S2|-|S1|}{|S2|} * 100 , \quad \text{Eq. 9, where:}$$

984 $REL.\Delta BIAS:$ Relative BIAS difference (in %)

985 S2: Mean Bias of the default version of GEM-Hydro
 986 S1: Mean Bias of the calibrated version of GEM-Hydro
 987 The equation of the standard deviation of the error is given below.

988 $STD = \sqrt{\frac{1}{N} * \sum_{i=1}^N (X_i - \bar{X})^2}$, Eq. 10, where:

989 STD: Standard deviation of the error

990 N: total number of observation-simulation pairs.

991 $X_i = P_i - O_i$, where P_i is the simulated (or forecasted) value for time-step i , and
 992 O_i is the observed value for time-step i .

993 As such, the standard deviation of the error can be seen as a measure of the variations of the
 994 model errors from which the mean bias would have been removed.

995 To compute the relative difference of the standard deviation of the error, Equation 11 below
 996 was used.

997 $REL.\Delta STDEV = \frac{S2-S1}{S2} * 100$, Eq. 11, where:

998 REL.ΔSTDEV: Relative difference of the standard deviation of the error (in
 999 %).

1000 S2: Standard deviation of the error of the default GEM-Hydro version

1001 S1: Standard deviation of the error of the calibrated GEM-Hydro version

1002

1003

1004 *Table 6: Comparison between the default and calibrated versions of GEM-Hydro with regard to surface variables.*
 1005 *TD: 2-m dew point temperature. TT: 2-m air temperature. UV: 10-m wind speed. Relative differences of the bias and*
 1006 *the standard deviation of the error between the two experiments are shown. Warm colors and positive values*
 1007 *denote an improvement of the calibrated version upon the default one, while cold colors and negative values denote*
 1008 *a degradation. Note that the relative differences are shown here for different periods. For the values split by season,*
 1009 *note that for each season, the average of the values for the years 2016 and 2017 is shown. See text for more details*
 1010 *on the computation of the relative differences shown here.*

		Period / variable	FULL	WINTER	SPRING	SUMMER	FALL
		20130101 / 20171231	0101-0331	0401-0630	0701-0930	1001-1231	
REL. ΔBIAS	TD	1.45%	1.06%	2.50%	1.30%	1.02%	
	TT	1.00%	-0.28%	1.40%	0.37%	0.15%	
	UV	-0.27%	0.12%	-0.49%	-0.41%	-0.17%	
REL. ΔSTDEV	TD	0.08%	-0.03%	0.13%	0.04%	0.01%	
	TT	-0.05%	-0.03%	-0.06%	0.02%	0.01%	
	UV	-0.02%	-0.01%	-0.04%	-0.04%	-0.02%	

1011

1012 It can be seen from Table 6 that the differences with regard to near-surface variables,
 1013 between the two versions of GEM-Hydro, are generally small, and can be considered neutral
 1014 in terms of the standard deviation of the error. A generally small improvement of the
 1015 calibrated upon the default version can be noticed for TT and TD Bias, while small degradations
 1016 are noticed for the wind speed. Note that regarding TT, the conclusions actually depend on
 1017 the season considered. Regarding wind speed, it is not exactly known why a small degradation
 1018 could occur with the calibrated version, especially when considering that the multiplying
 1019 coefficient related to surface roughness was not employed in this final calibration framework

1020 (see Methods). However, the UV bias differences are generally very small between the two
1021 versions, of the order of $0.015 \text{ m}\cdot\text{s}^{-1}$ (not shown here), which can be considered negligible. The
1022 same is true with regard to differences related to TT and TD. For example, the best
1023 improvement, which was noticed for the spring season and for TD Bias (Table 6), involves
1024 differences between the two GEM-Hydro versions of the order of $0.05 \text{ }^{\circ}\text{C}$. maximum (not
1025 shown here), which can also be considered negligible. Note, however, that the model has a
1026 tendency to overestimate TD by 1 to 2 $^{\circ}\text{C}$ during the day (local time corresponds to UTC -4
1027 hours during the spring period), over this region and for the spring season of 2017. However,
1028 when looking at the TD bias evolution as a function of the hour of the day but when considering
1029 the full period from January 1st 2013 to December 31st, 2017, this TD overestimation reaches
1030 1 $^{\circ}\text{C}$. maximum (not shown). Regarding 2-m air temperature (TT), GEM-Hydro simulations
1031 however have a tendency to underestimate this variable by about $0.5 \text{ }^{\circ}\text{C}$. during the night (not
1032 shown).

1033 **Usage notes**

1034 It is emphasized here that the gridded surface variables shared in this dataset
1035 correspond to outputs of the SVS model, which is the land surface scheme of the GEM-Hydro
1036 model. Therefore, these surface variables are valid over land only, and not over other types of
1037 continental surfaces, such as glaciers, water, or ice. However, the water (and ice) surfaces
1038 were neglected in the GEM-Hydro setup employed here, implying that most grid-cells of the
1039 region of interest (except inside big lakes such as the Great Lakes, for example) were assumed
1040 to be filled at 100% with land surfaces only. See the Methods' section (point 4.1) and the Data
1041 records' section for more information about this modelling choice. Despite of this, the surface
1042 fluxes shared in this dataset (including surface runoff, soil lateral flow, and soil base drainage)
1043 can still be used as inputs to any routing model implemented over a basin that is included in
1044 the region of interest, provided that this basin does not include grid-cells that are filled at
1045 100% with water surfaces: otherwise, the routing model will miss the fluxes coming from these
1046 100% water pixels. This can be ensured based on the "WT" variable shared in this dataset,
1047 which represents the percentage of the land surface that was considered inside each grid-cell
1048 (see Data Records), for the GEM-Hydro simulations performed here.

1049 In order to drive a routing model with the surface fluxes shared in this dataset, the
1050 sum of surface runoff and lateral flow (i.e. the "TRAF" and "ALAT" variables of this dataset)
1051 should be directly given as inputs to the surface network of the routing model (i.e. lakes and
1052 rivers), while the SVS soil base drainage (the "O1" variable) should be provided first to a
1053 baseflow model (i.e., a model representing the aquifer), that is sometimes already included in
1054 the routing model. Indeed, the "O1" variable represents the aquifer recharge. The aquifer
1055 model will then simulate the baseflow that returns to the surface network of lakes and rivers,
1056 in the routing model. Note that the units of these surface fluxes correspond to $\text{kg}/\text{m}^2/\text{h}$ or
1057 mm/h (assuming a density of $1000 \text{ kg}/\text{m}^3$, i.e. unsalted water). Therefore, when provided to a
1058 routing model, these fluxes should then be multiplied by a surface area (like the area of a
1059 subbasin or of the routing model grid-cell) in order to convert them into a volume of water
1060 per units of time. This is generally done in the routing model itself.

1061 Finally, it is reminded here that the SM variables of this dataset (the WSL1-6 variables)
1062 only represent the liquid soil moisture content of a given soil layer. However, the version of
1063 SVS used in this work did not represent soil freeze-thaw processes (more information in the
1064 Data Records' section), such the WSL1-6 variables still represent the total water stored in the
1065 different soil layers, in the GEM-Hydro simulations performed during this work.

1066 **Code Availability**

1067 The SVS land-surface scheme and the WATROUTE routing scheme are both available
1068 in the MESH official repository available at this address: <https://github.com/MESH->

1069 [Model/MESH-Releases](#) (accessed on February 1st, 2024). The Raven routing model is open-
1070 source and can be accessed here: [the Raven Hydrological Framework - Home Page](#)
1071 [\(uwaterloo.ca\)](#) (accessed on November 30, 2023). The DDS calibration algorithm is available
1072 in the Ostrich calibration toolkit and can be accessed here: [OSTRICH Optimization Software](#)
1073 [Toolkit \(uwaterloo.ca\)](#) (accessed on November 30, 2023). The MESH-SVS-Raven setups used
1074 in this study to calibrate the SVS and routing parameters may be shared upon reasonable
1075 request. GEM-Surf (the surface component of GEM-Hydro) is open-source and is available on
1076 Github: <https://github.com/ECCC-ASTD-MRD/sps.git> GEM-Surf can be run outside of ECCC
1077 informatic infrastructure. However, it still needs to rely on forcing and geophysical fields in the
1078 “standard file” format (a binary file format only used internally at ECCC), and produces output
1079 files in this format as well. Some tools needed to manipulate and read files of this format are
1080 also available on github: <https://github.com/ECCC-ASTD-MRD>

1081 Moreover, the WATROUTE version included in MESH cannot be run in a standalone
1082 mode, but only together with the SVS land-surface scheme included in MESH. The WATROUTE
1083 version used internally at ECCC cannot yet be run outside of ECCC infrastructure. Therefore, it
1084 is not yet possible to exactly replicate the GEM-Hydro simulations (i.e., by running GEM-
1085 Surf+WATROUTE) described here, outside of ECCC informatic infrastructure.

1087 **Acknowledgements**

1088 The authors wish to thank Dr. James Craig from the University of Waterloo, for his
1089 availability and support with regard to the use of the Raven routing model. The authors also
1090 wish to thank Dorothy Durnford from ECCC, for her strong involvement in the constant
1091 improvement of the WATROUTE model setups used at ECCC to simulate streamflow over
1092 Canada, including over the Great-Lakes and Ottawa River basins.

1094 **Author contributions**

1095 -Étienne Gaborit performed the calibration experiments with MESH-SVS-Raven, performed
1096 the GEM-Hydro simulations, processed the GEM-Hydro outputs, performed the streamflow
1097 evaluation and the near-surface variables’ evaluation, published the GEM-Hydro data on the
1098 Federated Research Data Repository (FRDR), and wrote the Data descriptor.

1099 -Juliane Mai performed the evaluation of the GEM-Hydro auxiliary hydrologic variables for all
1100 of the calibration trials involved during this work (Figure 9), and actively participated in the
1101 preparation of the Raven setups used in this study, and in the collection of the observed
1102 streamflow time-series and the reference datasets used to evaluate the auxiliary hydrologic
1103 variables (Table 5), which were inherited from the GRIP-GL project (Mai et al. 2022¹²).

1104 -Vincent Vionnet performed the comparison between GEM-Hydro and ERA-5 Land SWE biases
1105 (Figure 10), significantly contributed to improving the driver script used at ECCC to run GEM-
1106 Surf open-loop simulations, and performed a comprehensive review of this document.

1107 -Dan Princz performed the integration of the SVS code into the MESH Platform, and is the main
1108 lead developer of the MESH platform. He developed the MESH functionalities required to be
1109 able to couple MESH with the Raven routing model, as well as the scripts needed to convert a
1110 GEM-Hydro setup into a MESH-SVS(-WATROUTE) setup.

1111 -Hongren Shen was the main person responsible for the preparation of the Raven routing
1112 model setups used in this work and that were inherited from the GRIP-GL project (Mai et al.
1113 2022¹²).

1114 -Bryan Tolson was Hongren Shen and Juliane Mai’s supervisor at the time of the GRIP-GL
1115 project, and contributed significantly to many of the methodological choices made in the GRIP-
1116 GL project, which strongly influenced the methodology employed here.

1117 -Vincent Fortin is Étienne Gaborit’s supervisor and also contributed significantly to many
1118 methodological choices made during the GRIP-GL project and the resulting calibration trials
1119 that lead to the dataset described in this document.

1120

1121 **Competing interests**

1122 All of the authors of this data descriptor declare that they have not any conflict of interest with
1123 regard to the work and the data related to this document, or to the content of this document.
1124

1125 **References**

- 1126 1. Gaborit, É., et al. A hydrological prediction system based on the SVS land-surface
1127 scheme: efficient calibration of GEM-Hydro for streamflow simulation over the
1128 Lake Ontario basin. *Hydrol. Earth Syst. Sci.*, **21(9)**, 4825-4839.
1129 <https://doi.org/10.5194/hess-21-4825-2017> (2017)
- 1130 2. Vionnet, V., et al. Assessing the factors governing the ability to predict late-spring
1131 flooding in cold-region mountain basins. *Hydrol. Earth Syst. Sci.*, **24(4)**, 2141-2141
1132 (2020).
- 1133 3. Durnford, D., et al. Hydrological prediction systems at Environment and Climate
1134 Change Canada. *AMS 101st annual meeting*, January 9-15, 2021. Poster
1135 presentation (586) and extended abstract. Available at:
1136 <https://ams.confex.com/ams/101ANNUAL/meetingapp.cgi/Paper/383559>
- 1137 4. Baroni, G., et al. A comprehensive distributed hydrological modeling
1138 intercomparison to support process representation and data collection
1139 strategies. *Water Resour. Res.*, **55(2)**, 990-1010 (2019).
- 1140 5. Budhathoki, S., Rokaya, P., and Lindenschmidt, K. E. Improved modelling of a
1141 Prairie catchment using a progressive two-stage calibration strategy with in-situ
1142 soil moisture and streamflow data. *Hydrol. Res.*, **51(3)**, 505-520 (2020).
- 1143 6. Hirpa, F. A., et al. Calibration of the Global Flood Awareness System (GloFAS)
1144 using daily streamflow data. *J. Hydrol.*, **566**, 595-606 (2018).
- 1145 7. Mai, J. Ten strategies towards successful calibration of environmental models. *J.*
1146 *Hydrol.*, **620**, 129414 (2023).
- 1147 8. Bajracharya, A. R., Ahmed, M. I., Stadnyk, T., and Asadzadeh, M. Process based
1148 calibration of a continental-scale hydrological model using soil moisture and
1149 streamflow data. *J. Hydrol.: Regional Studies*, **47**, 101391 (2023).
- 1150 9. Mei, Y., et al. Can hydrological models benefit from using global soil moisture,
1151 evapotranspiration, and runoff products as calibration targets? *Water Resour.*
1152 *Res.*, **59(2)**, e2022WR032064 (2023).
- 1153 10. Demirel, M. C., et al. Tradeoffs between temporal and spatial pattern calibration and their
1154 impacts on robustness and transferability of hydrologic model parameters to ungauged
1155 basins. *Water Resour. Res.*, **60(1)**, e2022WR034193 (2024).
- 1156 11. Mai, J., et al. Great Lakes runoff intercomparison project phase 3: Lake Erie (GRIP-
1157 E). *J. Hydrol. Eng.*, **26(9)**, 05021020. [https://doi.org/10.1061/\(ASCE\)HE.1943-5584.0002097](https://doi.org/10.1061/(ASCE)HE.1943-5584.0002097) (2021).
- 1158
1159 12. Mai, J., et al. The Great Lakes runoff intercomparison project phase 4: the Great
1160 Lakes (GRIP-GL). *Hydrol. Earth Syst. Sci.*, **26**, 3537–3572.
1161 <https://doi.org/10.5194/hess-26-3537-2022> (2022).
- 1162 13. Gaborit, É. Hydrologic outputs from the 2023 calibrated version of GEM-Hydro
1163 over the Great-Lakes and Ottawa River region. Le Dépôt fédéré de données de
1164 recherche. Federated Research Data Repository (FRDR).
1165 <https://doi.org/10.20383/103.0847> (2024).

- 1166 14. Bernier, N. B., Bélair, S., Bilodeau, B., and Tong, L. Near-surface and land surface
1167 forecast system of the Vancouver 2010 winter Olympic and paralympic games. *J.*
1168 *Hydrometeorol.*, **12**, 508– 530. <https://doi.org/10.1175/2011JHM1250.1> (2011).
- 1169 15. Alavi, N., et al. Warm season evaluation of soil moisture prediction in the Soil,
1170 Vegetation and Snow (SVS) scheme. *J. Hydrometeorol.*, **17**, 2315–2332,
1171 <https://doi.org/10.1175/JHM-D-15-0189.1> (2016).
- 1172 16. Husain, S. Z., et al. The multi-budget Soil, Vegetation, and Snow (SVS) scheme for
1173 land surface parameterization: offline warm season evaluation. *J.*
1174 *Hydrometeorol.*, **17**, 2293–2313, <https://doi.org/10.1175/JHM-D-15-0228.1>
1175 (2016).
- 1176 17. Leonardini, G., et al. Evaluation of the Soil, Vegetation, and Snow (SVS) land
1177 surface model for the simulation of surface energy fluxes and soil moisture under
1178 snow-free conditions. *Atmosphere*, **11(3)**, 278,
1179 <https://doi.org/10.3390/atmos11030278> (2020).
- 1180 18. Leonardini, G., F. Anctil, V. Vionnet, M. Abrahamowicz, D. F. Nadeau, and V.
1181 Fortin. Evaluation of the snow cover in the Soil, Vegetation, and Snow (SVS) land
1182 surface model. *J. Hydrometeorol.*, **22**, 1663–1680, <https://doi.org/10.1175/JHM-D-20-0249.1> (2021).
- 1183 1184 19. Kouwen, N. *WATFLOOD/WATROUTE Hydrological Model Routing & Flow*
1185 *Forecasting System*. Department of Civil Engineering, University of Waterloo,
1186 Waterloo, ON, 267 pp. 2010.
- 1187 20. Yassin, F., Razavi, S., Elshamy, M., Davison, B., Sapriza-Azuri, G., and Wheeler, H.
1188 Representation and improved parameterization of reservoir operation in
1189 hydrological and land-surface models. *Hydrol. Earth Syst. Sci.*, **23(9)**, 3735-3764
1190 (2019).
- 1191 21. Gaborit, É., Fortin, V., and Durnford, D. On the implementation of the
1192 dynamically zoned target release reservoir model in the GEM-Hydro streamflow
1193 forecasting system. *Can. J. Civ. Eng.*, **49(10)**: 1582-
1194 1594, <https://doi.org/10.1139/cjce-2021-0507>, (2022).
- 1195 22. Pietroniro, A., et al. Development of the MESH modelling system for hydrological
1196 ensemble forecasting of the Laurentian Great Lakes at the regional scale. *Hydrol.*
1197 *Earth Syst. Sci.*, **11(4)**, 1279-1294 (2007).
- 1198 23. Craig, J. R., et al. Flexible watershed simulation with the Raven hydrological
1199 modelling framework. *Environ. Model. Soft.*, **129**, 104728 (2020).
- 1200 24. Gasset, N., et al. A 10 km North American precipitation and land-surface
1201 reanalysis based on the GEM atmospheric model. *Hydrol. Earth Syst. Sci.*, **25(9)**,
1202 4917-4945 (2021).
- 1203 25. Garnaud, C., et al. Improving snow analyses for hydrological forecasting at ECCC
1204 using satellite-derived data. *Remote Sens.*, **13**, 5022,
1205 <https://doi.org/10.3390/rs13245022> (2021).
- 1206 26. Gaborit, É., Ricard, S., Lachance-Cloutier, S., Anctil, F., and Turcotte, R. Comparing
1207 global and local calibration schemes from a differential split-sample test
1208 perspective. *Can. J. Earth Sci.*, **52(11)**, 990-999, <https://doi.org/10.1139/cjes-2015-0015>
1209 (2015).

- 1210 27. Tolson, B. A., and Shoemaker, C. A. Dynamically dimensioned search algorithm
1211 for computationally efficient watershed model calibration. *Water Resour.*
1212 *Res.*, **43(1)** (2007).
- 1213 28. Kling, H., Fuchs, M., and Paulin, M. Runoff conditions in the upper Danube basin
1214 under an ensemble of climate change scenarios. *J. Hydrol.*, **424**, 264-277 (2012).
- 1215 29. De Schepper, G., Therrien, R., Refsgaard, J. C., and Hansen, A. L. Simulating
1216 coupled surface and subsurface water flow in a tile-drained agricultural
1217 catchment. *J. Hydrol.*, **521**, 374-388 (2015).
- 1218 30. Harder, P., and Pomeroy, J. Estimating precipitation phase using a psychrometric
1219 energy balance method. *Hydrol. Process.*, **27(13)**, 1901-1914 (2013).
- 1220 31. Vionnet, V., et al. Snow level from post-processing of atmospheric model
1221 improves snowfall estimate and snowpack prediction in mountains. *Water*
1222 *Resour. Res.*, **58(12)**, e2021WR031778 (2022).
- 1223 32. USGS: USGS EROS archive- Digital Elevation- Global Multi-resolution Terrain
1224 Elevation Data 2010 (GMTED 2010), <https://doi.org/10.5066/F7J38R2N>, (2010).
1225 Accessed: 2023-12-05.
- 1226 33. ESA: Land Cover CCI vegetation cover,
1227 <http://maps.elie.ucl.ac.be/CCI/viewer/download.php> (2015), accessed: 2023-12-
1228 05.
- 1229 34. Shangguan, W., Dai, Y., Duan, Q., Liu, B., and Yuan, H. A global soil dataset for
1230 earth system modeling. *J. Adv. Model. Earth Syst.*, **6**, 249–263,
1231 <https://doi.org/10.1002/2013MS000293> (2014).
- 1232 35. Natural Resources Canada: National hydro network—NHN—Geobase series,
1233 [https://open.canada.ca/data/en/dataset/a4b190fe-e090-4e6d-881e-
1234 b87956c07977](https://open.canada.ca/data/en/dataset/a4b190fe-e090-4e6d-881e-b87956c07977) (2020), accessed: 2021-03-03.
- 1235 36. USGS: National Hydrography Dataset, [https://www.usgs.gov/core-science-
1236 systems/ngp/national-hydrography/national-hydrography-dataset](https://www.usgs.gov/core-science-systems/ngp/national-hydrography/national-hydrography-dataset) (2021),
1237 accessed: 2023-12-05.
- 1238 37. HydroSHEDS: HydroSHEDS website, <https://www.hydrosheds.org/> (2021),
1239 accessed: 2023-12-05
- 1240 38. Mohammed, A. A., Kurylyk, B. L., Cey, E. E., and Hayashi, M. Snowmelt infiltration
1241 and macropore flow in frozen soils: Overview, knowledge gaps, and a conceptual
1242 framework. *Vadose Zone J.*, **17(1)**, 1-15 (2018).
- 1243 39. Nash, J. E., and Sutcliffe, J. V. River flow forecasting through conceptual models
1244 part I—A discussion of principles. *J. Hydrol.*, **10(3)**, 282-290 (1970).
- 1245 40. Kirchner, J. W. Getting the right answers for the right reasons: Linking
1246 measurements, analyses, and models to advance the science of hydrology. *Water*
1247 *Resour. Res.*, **42(3)** (2006).
- 1248 41. Beven, K., and Binley, A. The future of distributed models: model calibration and
1249 uncertainty prediction. *Hydrol. Process.*, **6(3)**, 279-298 (1992).
- 1250 42. Gupta, H. V., Kling, H., Yilmaz, K. K., and Martinez, G. F. Decomposition of the
1251 mean squared error and NSE performance criteria: Implications for improving
1252 hydrological modelling. *J. Hydrol.*, **377(1-2)**, 80-91 (2009).

- 1253 43. Tong, C., et al. Soil moisture retrievals by combining passive microwave and optical
1254 data. *Remote Sens.* **12**, 3173, <https://doi.org/10.3390/rs12193173> (2020).
- 1255 44. Martens, B., et al. GLEAM v3: satellite-based land evaporation and root-zone soil
1256 moisture, *Geosci. Model Dev.*, **10**, 1903–1925 (2017).
- 1257 45. Muñoz Sabater, J. ERA5-Land hourly data from 1981 to present. Copernicus
1258 Climate Change Service (C3S) Climate Data Store (CDS),
1259 <https://doi.org/10.24381/cds.e2161bac> (2019). Accessed on 2023-12-05.
- 1260 46. Vionnet, V., Mortimer, C., Brady, M., Arnal, L., and Brown, R. Canadian historical
1261 snow water equivalent dataset (CanSWE, 1928–2020). *Earth Syst. Sci. Data*, **13(9)**,
1262 4603-4619 (2021).
- 1263 47. Mortimer, C., et al. Benchmarking algorithm changes to the snow CCI+ snow water
1264 equivalent product. *Remote Sensing of Environment*, **274**, 112988,
1265 <https://doi.org/10.1016/j.rse.2022.112988> (2022).
- 1266
- 1267
- 1268

